^{31}P (proton-coupled) NMR δ 232.3 (dt, J_{PH} = 362 Hz, $J_{PP'}$ = 59 Hz, *P*HPh), 15.2 (d, $J_{PP'}$ = 59 Hz). Anal. Calcd for $WC_{23}H_{45}P_3Cl_2$: C, 41.28; H, 6.78. Found: C, 41.71; H, 6.82.

Crystal Structure Determination. A. Data Collection. Deep red plate-like crystals of $W(CCMe_3)(PHPh)(PEt_3)_2Cl_2$ were grown from toluene. A crystal measuring approximately 0.24 × 0.24 × 0.32 mm was sealed into a glass capillary under inert-atmospheric conditions. Description of our use of the Syntex $P2_1$ diffractometer has been published;[30] details pertaining to the present analysis are in Table II. Systematic absences observed were $h0l$ for $h = 2n + 1$ and $0kl$ for $k + l = 2n + 1$; possible space groups are the noncentrosymmetric orthorhombic space group $Pna2_1$ (C_{2v}^9 No. 33) or the centrosymmetric space group $Pnam$ (a nonstandard setting of $Pnma$—D_{2h}^{16}; No. 62).

In view of the possibility of the noncentrosymmetric space group $Pna2_1$ (with polar c axis), intensity data were collected for the two forms hkl and $hk\bar{l}$. The intensity data were corrected for absorption by using the empirical ψ-scan method with seven reflections covering the 2θ range 19–45°.

B. Solution and Refinement. The structure was initially solved in the acentric space group $Pna2_1$ by Patterson and difference-Fourier techniques, which determined the coordinates of all non-hydrogen atoms. Full-matrix least-squares refinement led to R_F = 4.8%. However, unreasonably large C–C distances within the PEt_3 ligands, coupled with the appearance of mirror symmetry within the molecule, led us to attempt further refinement in the higher symmetry centric space group $Pnam$; this choice proved to be correct as verified by successful refinement and chemically reasonable features throughout the molecule. Difference-Fourier calculations failed to locate the unique P-bonded hydrogen atom; all other hydrogen atoms were included in calculated positions.[31] The final agreement factors were R_F = 2.8%, R_{wF} = 2.9%, and GOF = 1.01 for all 2007 point-group independent data with $4.0 \leq 2\theta \leq 50.0°$ (none rejected). The ratio of observations to variables was 2007:151 = 13.3:1. Structure factor calculations excluding data with $|F_o| < 3\sigma(|F_o|)$ gave R_F = 2.4%, R_{wF} = 2.8%, and GOF = 0.99.

Final positional parameters are listed in Table III.

Acknowledgment. This work was generously supported by the National Science Foundation through Grants CHE 80 23448 (M.R.C.) and CHE 79 05307 (R.R.S.).

Registry No. $W(O)(CHCMe_3)(PEt_3)_2Cl_2$, 74666-77-6; $[NEt_4][W(CCMe_3)Cl_4]$, 78251-20-4; $W(CCMe_3)(NHPh)(PEt_3)_2Cl_2$, 82661-13-0; $W(CCMe_3)(NHPh)(PMe_2Ph)_2Cl_2$, 82661-14-1; $W(CCMe_3)(NHPh)(PEt_3)Cl_2$, 82661-15-2; $W(CCMe_3)(PEt_3)Cl_3$, 82661-16-3; $W(CCMe_3)(NPh)(PEt_3)_2Cl$, 82661-17-4; $Ph_3P{=}CH_2$, 3487-44-3; $W(CCMe_3)(NH_2)(PEt_3)_2Cl_2$, 82661-18-5; $W(CCMe_3)(PHPh)(PEt_3)_2Cl_2$, 82661-19-6.

Supplementary Material Available: Listings of observed and calculated structure factor amplitudes, positional parameters for hydrogen atoms (Table I-S), and anisotropic thermal parameters (Table II-S) (14 pages). Ordering information is given on any current masthead page.

---

[30] Churchill, M. R.; Lashewycz, R. A.; Rotella, F. J. *Inorg. Chem.* 1977, *16*, 265.

[31] Churchill, M. R. *Inorg. Chem.* **1973**, *12*, 1213.

Photochemistry of Solution and Surface-Confined Alkyl- and Benzyltricarbonylcyclopentadienyltungsten Complexes

Bernard Klein, Romas J. Kazlauskas, and Mark S. Wrighton*

Department of Chemistry, Massachusetts Institute of Technology, Cambridge, Massachusetts 02139

Received May 20, 1982

A variety of surface-confined species $(\eta^5\text{-}C_5H_5)W(CO)_3R$ (R = Cl, CH_3, C_2H_5, $CH_2C_6H_5$) has been synthesized and characterized and their photochemistry examined and compared to solution analogues. High surface area (400 m^2/g) SiO_2, $[SiO_2]$–, has been functionalized first with $–SiMe_2C_5H_5$ by reaction of surface OH groups with $ClSiMe_2C_5H_5$ or $EtOSiMe_2C_5H_5$. The resulting $[SiO_2]–SiMe_2C_5H_5$ can then be treated in a series of conventional synthetic steps to yield $[SiO_2]–SiMe_2–(\eta^5\text{-}C_5H_4)W(CO)_3R$ (R = Cl, CH_3, C_2H_5). Elemental analyses and infrared spectroscopy has been used to establish that the average coverage is generally submonolayer, with an average separation between W centers of 10–20 Å. Chloromethylated polystyrene reacts with $[(\eta^5\text{-}C_5H_5)W(CO)_3]^-$ to yield $(\eta^5\text{-}C_5H_5)W(CO)_3(\eta^1\text{-}CH_2C_6H_4–[P])$ or with C_5H_5Na followed by conventional synthetic procedures to yield $[P]–C_6H_4CH_2–(\eta^5\text{-}C_5H_4)W(CO)_3R$ (R = CH_3, C_2H_5). In all cases near-UV (355 nm) irradiation yields chemistry consistent with efficient, dissociative loss of CO as the primary reaction following photoexcitation as has been found for the analogous solution species ($\Phi_{366} \approx 0.35 \pm 0.05$). Direct spectroscopic evidence for the photogeneration of surface-confined, 16-valence-electron intermediates comes from the infrared analysis of Nujol suspensions of $[SiO_2]–SiMe_2–(\eta^5\text{-}C_5H_4)W(CO)_3R$ (R = CH_3, C_2H_5) irradiated at 77 K. For R = CH_3 warm-up of the irradiated sample yields nearly complete regeneration of the starting complex by back-reaction with the photoejected CO, whereas for R = C_2H_5 warm-up yields some regeneration of the starting complex and some conversion to $[SiO_2]–SiMe_2–(\eta^5\text{-}C_5H_4)W(CO)_2(H)(C_2H_4)$. Unlike the analogous complex in solution, prolonged irradiation of the $[SiO_2]–SiMe_2–(\eta^5\text{-}C_5H_4)W(CO)_3R$ does not yield W–W bonded products, consistent with the immobilized centers remaining anchored sufficiently far apart that W–W bonds cannot form. Irradiation of $(\eta^5\text{-}C_5H_5)W(CO)_3(\eta^1\text{-}CH_2C_6H_4–[P])$ at 77 K does not allow the observation of a 16-valence-electron intermediate rather $(\eta^5\text{-}C_5H_5)W(CO)_2(\eta^3\text{-}CH_2C_6H_4\text{-}[P])$ is formed. These and similar results for the solution species R = $CH_2C_6H_5$ and $CH(CH_3)C_6H_5$ allow an upper limit for the activation energy for the conversion of an η^1-benzyl to η^3-benzyl to be set at ~6 kcal/mol. Irradiation of $(\eta^5\text{-}C_5H_5)W(CO)_3CH_2CH_2C_6H_5$ leads to a blue 16-valence-electron species at 77 K which gives *trans*-$(\eta^5\text{-}C_5H_5)W(CO)_2(H)$(styrene) upon warming. This styrene–hydride rearranges slowly at 300 K ($t_{1/2}$ = ~400 s) to form $(\eta^5\text{-}C_5H_5)W(CO)_2(\eta^3\text{-}CH(CH_3)C_6H_5)$.

Surface-confined organometallic species have recently received widespread attention[1–7] and have been the subject of two recent reviews.[1,2] The interest in these materials is due to their potential ability to effect catalysis of numerous reactions. Indeed, they are sometimes referred to as "third generation catalysts",[2] for they include advantages of both previously known homo- and heterogeneous catalysts: (1) they are easily removed from the reaction medium and present good mechanical stability; (2) the surface-confined sites are well-defined and are reproducibly prepared, whereas the activity of heterogeneous catalysts is often irreproducible; (3) the surface-confined catalyst has normally one type of active site, thus providing high specificity; (4) any solvent can be used in the reaction, whereas the utility of homogeneous catalysts is sometimes limited by the solubility of the catalysts; (5) and surface-confined species are sometimes more durable than their homogeneous analogues. In addition, the decomposition of surface-anchored organometallics can yield highly active dispersed metal oxide particles, which are also very effective in catalysis.[8]

Work done in this area has employed two classes of supports: inorganic oxides and organic polymers. Although there is a wide variety in methods of surface anchoring, much of the published data deals with organometallics attached through a surface-bound phosphine ligand. Organometallics attached through a functionalized cyclopentadienyl ring have been reported for Cr, Mo, W,[3,4] Fe, Co,[5] Rh,[6] and Ti.[7]

Photochemistry of surface-confined molecules is not a well-developed field. However, recent studies of the photochemistry of surface-confined $SiCo(CO)_4$,[9,10] $L_3Ru_3(CO)_9$,[11] $LRu(CO)_4$,[11] and $LFe(CO)_4$[12] have shown that the surface reactions can be monitored with molecular specificity by using Fourier transform infrared (FTIR)[11,12] transmission or photoacoustic spectroscopy (FTIR/PAS).[9] As in photoexcitation of any chemical system, the optical energy can be selectively deposited into a given chemical constituent, depending on the absorption properties. While the photochemistry of appropriate solution species[13] can be used as a guide to the photochemistry of the surface-confined species, the support may alter the primary photochemical events and thermal reactions of primary products. Further, the fact that the photoexcited species and possibly the product(s) are immobilized can prevent certain processes requiring diffusion. Photochemistry of surface-confined molecules may have practical importance in imaging, catalysis, and weathering and corrosion inhibition, in addition to providing new insights into reaction mechanisms.

If photochemical reactions are carried out at low temperatures, it is sometimes possible to accumulate and characterize intermediates which would otherwise react rapidly to give further products. These techniques have been recently applied to identify intermediates in β-hydrogen transfer reactions of 16-valence electron $(\eta^5\text{-}C_5H_5)W(CO)_3R$ (where R has β-hydrogens) which are generated by photoinduced dissociative loss of CO from the parent compound $(\eta^5\text{-}C_5H_5)W(CO)_3R$.[14] The subsequent thermal transformation shown in eq 1 takes place

$$\underset{\text{16-e species}}{(\eta^5\text{-}C_5H_5)W(CO)_2C_2H_5} \xrightarrow{\Delta} \underset{\text{18-e species}}{trans\text{-}(\eta^5\text{-}C_5H_5)W(CO)_2H(C_2H_4)} \quad (1)$$

in a series of steps involving weakening of the β-C–H bond and complete transfer to form the cis-$(\eta^5\text{-}C_5H_5)W(CO)_2(H)(C_2H_4)$ followed by rate-determining cis to trans isomerization.[14]

In this paper we report the synthesis and photochemical characterization of a variety of surface-confined $(\eta^5\text{-}C_5H_5)W(CO)_3R$ species. Supports used are high surface area SiO_2, $[SiO_2]$–, and chloromethylated polystyrene, $[P]\text{–}C_6H_4CH_2\text{–}$, and the species have been anchored either via functionalization of the $\eta^5\text{-}C_5H_5$ ring or the R group of the complex. In every case the photochemistry is consistent with dissociative loss of CO, eq 2, as the primary photoproduct, as found for such species in homogeneous solution.[14,15]

$$\text{surface–}[(\eta^5\text{-}C_5H_5)W(CO)_3R] \xrightarrow{h\nu} \text{surface–}[(\eta^5\text{-}C_5H_5)W(CO)_2R] + CO \quad (2)$$

The surface supported 16-valence-electron species can in some cases be characterized at low temperatures and undergo reactions upon warming, paralleling the solution species. Reactions such as ligand addition, β-hydrogen transfer, and conversion of an η^1-benzyl to an η^3-benzyl have been observed for supported species. However, the immobilized 16-valence electron species formed by photoejection of CO do not lead to dinuclear metal complexes on the surface in contrast to the net result from irradiation of appropriate solution species.

Experimental Section

Materials. Tetrahydrofuran (THF) was freshly distilled from Na/benzophenone under N_2. Hexane and toluene were freshly distilled from CaH_2 under N_2. Isooctane was purified according to previously reported procedures[14] and distilled from CaH_2 under N_2. Ether and Et_2O (Analytical Reagent grade, Mallinckrodt) was used as received. PPh_3 (99%, Aldrich) was recrystallized three

---

(1) Bailey, D. C.; Langer, S. H. *Chem. Rev.* **1981**, *81*, 109.

(2) Hartley, F. R.; Verey, P. N. *Adv. Organomet. Chem.* **1977**, *15*, 189.

(3) Gubitosa, G.; Brintzinger, H. H. *J. Organomet. Chem.* **1977**, *140*, 127. Pittman, C. U., Jr.; Kim, B. T.; Douglas, W. M. *J. Org. Chem.* **1975**, *40*, 590. Awl, R. A.; Frankel, E. N.; Frederick, J. P.; Pride, E. H. *J. Am. Chem. Soc.* **1978**, *100*, 577. Tsouris, G. P.; Farana, M. F. *J. Organomet. Chem.* **1976**, *114*, 293. Macomber, D. W.; Rausch, M. D.; Tayanaman, T. V.; Puresher, R. D.; Pittman, C. U., Jr. *Ibid.* **1981**, *205*, 353.

(4) Warel, S.; Buschmeyer, P. *Angew. Chem., Int. Ed. Engl.* **1978**, *17*, 131.

(5) Gubitosa, G.; Brintzinger, H. H. *J. Am. Chem. Soc.* **1977**, *99*, 5174. Wold, F. R. W. P.; Gubitosa, G.; Brintzinger, H. H. *J. Organomet. Chem.* **1978**, *148*, 73. Perkins, P.; Vallband, K. P. C. *J. Am. Chem. Soc.* **1979**, *101*, 3985. Arzoumanian, H.; Alvarez, R. L.; Kowalak, A. D.; Metzger, J. *Ibid.* **1977**, *99*, 5174.

(6) Tung, H. S.; Brubaker, C. H., Jr. *J. Organomet. Chem.* **1981**, *216*, 129. Chang, B. H.; Grubbs, R. H.; Brubaker, C. H., Jr. *Ibid.* **1979**, *172*, 81.

(7) Grubbs, R. H.; Biggons, C.; Krall, L. C.; Brends, W. D., Jr.; Brubacker, C. H., Jr. *J. Am. Chem. Soc.* **1973**, *95*, 2373. Bands, W. D., Jr.; Brubacker, C. H., Jr.; Chandrasekanan, E. S.; Gibbons, C.; Grubbs, R. H.; Kroll, L. C. *Ibid.* **1975**, *97*, 2128. Jackson, R.; Ruddlester, J.; Thompson, D. D.; Whelan, R. *J. Organomet. Chem.* **1977**, *125*, 57.

(8) Collman, J. P.; Hegedus, L. S.; Cooke, M. P.; Norton, J. R.; Dolcetti, G.; Marquardt, D. N. *J. Am. Chem. Soc.* **1972**, *94*, 1789. Ichikowa, M. J. *J. Chem. Soc., Chem. Commun.* **1976**, 11. Anderson, J. R.; Mainwaring, D. E. *J Catal.* **1974**, *35*, 162. Iwatabe, K.; Dasgupta, S. R.; Schneider, R. L.; Smith, G. C.; Watters, K. L. *Inorg. Chim. Acta* **1975**, *15*, 191.

(9) Kinney, J. B.; Staley, R. H.; Reichel, C. L.; Wrighton, M. S. *J. Am. Chem. Soc.* **1981**, *103*, 4273.

(10) Reichel, C. L.; Wrighton, M. S. *J. Am. Chem. Soc.* **1981**, *103*, 7180.

(11) Liu, D. K.; Wrighton, M. S. *J. Am. Chem. Soc.* **1982**, *104*, 898.

(12) Mitchener, J. C.; Wrighton, M. S. to be submitted for publication.

(13) Geoffroy, G. L.; Wrighton, M. S. "Organometallic Photochemistry"; Academic Press: New York, 1979.

(14) R = CH_3, C_2H_5, and n-pentyl: Kazlauskas, R. J.; Wrighton, M. S. *J. Am. Chem. Soc.* **1980**, *102*, 1727; *J. Am. Chem. Soc.*, in press.

(15) R = Cl: Alaway, D. G.; Barnett, K. W. *Inorg. Chem.* **1980**, *19*, 1533. R = CH_3 and $CH_2C_6H_5$: Severson, R. G.; Wojcicki, A. *J. Organomet. Chem.*, **1978**, *157*, 173. R = CH_3: Tyler, D. R. *Inorg. Chem.* **1981**, *20*, 2257. Alt, H. G. *J. Organomet. Chem.* **1977**, *124*, 167. R = C_2H_5: Alt, H. G.; Eichner, M. E. *Ibid.* **1981**, *212*, 397; *Angew. Chem., Int. Ed. Engl.* **1982**, *21*, 78. R = C_2H_4Ph: Su, S. C. H.; Wojcicki, A. Abstract 1C08 Tenth International Organometallic Chemistry Conference, Toronto, Canada, Aug 1981, p 47. This last reference describes preliminary results paralleling those described here.

Table I. Spectral Data for Relevant Compounds[a]

compd	IR, cm^{-1} (ϵ, M^{-1} cm^{-1}, or rel int)	UV-vis, nm (ϵ, M^{-1} cm^{-1})
$(\eta^5\text{-}C_5H_5)W(CO)_3CH_3$	2021 (6200), 1932 (13 600)	350 (sh), 310 (2500), 256
$[SiO_2]\text{-}SiMe_2\text{-}(\eta^5\text{-}C_5H_4)W(CO)_3CH_3$	2020 (1.0), 1934 (1.5)	350, 292, 248
$[P]\text{-}C_6H_4CH_2\text{-}(\eta^5\text{-}C_5H_4)W(CO)_3CH_3$	2009 (1.0), 1913 (1.6)	359, 303, 254
$(\eta^5\text{-}C_5H_5)W(CO)_2CH_3$ [b]	1955 (1.0), 1865 (1.0)	600
$[SiO_2]\text{-}SiMe_2\text{-}(\eta^5\text{-}C_5H_4)W(CO)_2CH_3$ [c]	1950 (1.0), 1859 (0.9)	
$(\eta^5\text{-}C_5H_5)W(CO)_2(PPh_3)CH_3$	1936 (1.0), 1861 (1.2)	
$[SiO_2]\text{-}SiMe_2\text{-}(\eta^5\text{-}C_5H_4)W(CO)_2(PPh_3)CH_3$	1938 (1.0), 1854 (2.0)	
$(\eta^5\text{-}C_5H_5)W(CO)_3C_2H_5$	2018 (6000), 1927 (9800)	348 (sh), 310 (2400), 250 (sh)
$[SiO_2]\text{-}SiMe_2\text{-}(\eta^5\text{-}C_5H_4)W(CO)_3C_2H_5$	2010 (1.0), 1920 (1.4)	358, 303
$[P]\text{-}C_6H_4CH_2\text{-}(\eta^5\text{-}C_5H_4)W(CO)_3C_2H_5$	2010 (1.0), 1920 (1.6)	360, 311, 248
$(\eta^5\text{-}C_5H_5)W(CO)_2C_2H_5$ [b]	1952 (1.0), 1865 (0.8)	565, 405
$[SiO_2]\text{-}SiMe_2\text{-}(\eta^5\text{-}C_5H_4)W(CO)_2C_2H_5$ [c]	1956 (1.0), 1853 (0.8)	
$(\eta^5\text{-}C_5H_5)W(CO)_2(PPh_3)C_2H_5$	1936 (2400), 1858 (7300)	380 (sh, 1600), 315 (sh, 4600), 260 (sh, 8600)
$[SiO_2]\text{-}SiMe_2\text{-}(\eta^5\text{-}C_5H_4)W(CO)_2(PPh_3)C_2H_5$	1922 (1.0), 1844 (~0.8)	
$(\eta^5\text{-}C_5H_5)W(CO)_2(H)(C_2H_4)$	1980 (1.0), 1905 (2.0)	~350 (sh)
$[SiO_2]\text{-}SiMe_2\text{-}(\eta^5\text{-}C_5H_4)W(CO)_2(H)(C_2H_4)$	1969 (1.0), 1892 (1.5)	
$(\eta^5\text{-}C_5H_5)W(CO)_3(\eta^1\text{-}CH_2C_6H_5)$	2017 (6900), 1934 (6000), 1927 (7000)	370 (sh, 1100), 301 (12 200), 262 (sh, 10 200)
$(\eta^5\text{-}C_5H_5)W(CO)_3(\eta^1\text{-}CH_2C_6H_4)\text{-}[P]$	2007 (1.0), 1915 (1.0)	360, 303, 254
$(\eta^5\text{-}C_5H_5)W(CO)_2(\eta^3\text{-}CH_2C_6H_5)$ [b]	1939 (1.0), 1863 (0.8)	~405
$(\eta^5\text{-}C_5H_5)W(CO)_2(\eta^3\text{-}CH_2C_6H_4)\text{-}[P]$	1934 (1.0), 1847 (1.6)	
$(\eta^5\text{-}C_5H_5)W(CO)_2(PPh_3)(\eta^1\text{-}CH_2C_6H_5)$	1928 (1.0), 1845 (~0.7)	
$(\eta^5\text{-}C_5H_5)W(CO)_3CH_2CH_2C_6H_5$	2016 (4900), 1925 (7300)	345 (sh, 1400), 312 (2500), 262 (16 000)
$(\eta^5\text{-}C_5H_5)W(CO)_2CH_2CH_2C_6H_5$ [b]	1939 (1.0), 1846 (0.9)	565, ~430 (sh)
$(\eta^5\text{-}C_5H_5)W(CO)_2(PPh_3)CH_2CH_2C_6H_5$ [d]	1923 (1.0), 1844 (0.7)	
$(\eta^5\text{-}C_5H_5)W(CO)_2(H)(\text{styrene})$	1975 (1.0), 1903 (1.6)	
$(\eta^5\text{-}C_5H_5)W(CO)_3(\eta^1\text{-}CH(CH_3)C_6H_5)$	2010 (6300), 1928 (4800), 1918 (7500)	380 (sh, 1100), 308 (11 200), 260 (sh, 9800)
$(\eta^5\text{-}C_5H_5)W(CO)_2(PPh_3)(\eta^1\text{-}CH(CH_3)C_6H_5)$ [d]	1936 (1.0), 1842 (~0.8)	
$(\eta^5\text{-}C_5H_5)W(CO)_2(\eta^3\text{-}CH(CH_3)C_6H_5)$	1942 (1.0), 1866 (0.8)	~420
$(\eta^5\text{-}C_5H_5)W(CO)_3Cl$	2050, 1965[e]	457 (530), 312 (2700)[f]
$[SiO_2]\text{-}SiMe_2\text{-}(\eta^5\text{-}C_5H_4)W(CO)_3Cl$	2047 (1.0), 1968 (1.0), 1948 (1.8)	472
$(\eta^5\text{-}C_5H_5)W(CO)_2(PPh_3)Cl$	1965, 1870[e]	
$[SiO_2]\text{-}SiMe_2\text{-}(\eta^5\text{-}C_5H_4)W(CO)_2(PPh_3)Cl$	1952 (1.0), 1870 (1.6)	

[a] All data for solution species were obtained in isooctane or methylcyclohexane at 300 K unless otherwise noted. Surface-supported species IR spectra were obtained as KBr pellets at 300 K. UV-vis spectra for surface-supported species were obtained by using photoacoustic spectroscopy at 300 K with carbon black as a reference. [b] Spectra obtained in methylcyclohexane at 77 K. [c] Spectra obtained as a Nujol mull at 77 K. [d] Spectra obtained in toluene containing 0.5 M PPh_3. [e] Chloroform solution. Data taken from: Alway, D. G.; Barnett, K. W. *Inorg. Chem.* **1980**, *19*, 1533. [f] Benzene solution. Data taken from the reference in footnote *e* above.

times from absolute ethanol. Chloromethylated polystyrene (1% divinylbenzene cross-linked, 0.32 mequiv of Cl/g) was obtained from Polyscience, Inc., and used as received. Cyclopentadienylmethylpolystyrene (20% DVB cross-linked; 90 mequiv of Cp/g) was also obtained from Polyscience, Inc., and used as received. High surface area SiO_2 (400 m^2/g, Alfa) was dried for 1 h at 250 °C and then for 16 h at 120 °C under 4×10^{-2} torr vacuum, and consequently showed an IR absorption at 3692 cm^{-1}, attributable to isolated or paired surface hydroxyl groups.[16] Sodium cyclopentadienide–dimethoxyethane adduct, $Na(C_5H_5)\cdot DME$ was available from previous work.[17] Elemental analyses were performed by Analytische Laboratorien, West Germany.

Instrumentation. UV–vis absorption spectra were recorded by using a Cary 17 spectrophotometer. For surface-confined materials, IR spectra were taken as KBr pellets (2–3% by mass silica or polymer) or as Nujol mulls between CaF_2 plates, on a Nicolet 7199 Fourier transform infrared spectrometer. Solution spectra were recorded by either using the FTIR or using a Perkin-Elmer 180 spectrometer. Low-temperature IR spectra were obtained by using a Precision Cell, Inc. Model P/N 21.000 variable-temperature cell with outer NaCl or CaF_2 windows, using liquid N_2 as coolant. NMR spectra were obtained by using a Varian T60 continuous-wave or JEOL FX90Q Fourier transform spectrometer. All chemical shifts are referenced to tetramethylsilane at 0 ppm. A Mel-Temp melting point apparatus was used to determine melting points of samples in capillaries under air and are uncorrected. FTIR/PAS spectra were obtained by using a Nicolet 7199 spectrometer, equipped with a photoacoustic detector[18] that allows control of the sample environment. The acoustic coupling gas was either 1 atm of Ar (<1 ppm H_2O, O_2) or 1 atm of a 1:4 mixture of O_2 and Ar (<1 ppm H_2O) for photolysis experiments. UV–vis photoacoustic spectra were recorded on a Princeton Applied Research Model 6001 photoacoustic spectrometer, using air as a coupling gas and carbon black as a reference. All manipulations of air-sensitive compounds were done under N_2 by using a Vacuum Atmospheres He-43-6 Dri-Lab glovebox with an attached He 493 Dri-Train or under Ar by using conventional Schlenk techniques.

$(\eta^5\text{-}C_5H_5)W(CO)_3R$. The complexes where R = Cl, CH_3, C_2H_5, and $n\text{-}C_5H_{11}$ were available from previous work.[14] The complexes where R = $CH_2C_6H_5$, $CH_2CH_2C_6H_5$, and $CH(CH_3)C_6H_5$ were prepared similarly[14] by reacting $(\eta^5\text{-}C_5H_5)W(CO)_3Na$ in THF with benzyl bromide, 1-bromo-2-phenylethane, or 1-bromo-1-phenylethane, respectively, and purified by recrystallization from hexane. All are crystalline, air-stable, yellow species. IR and UV–vis data are listed in Table I. Melting points (uncorrected): $CH_2C_6H_5$, 97–98 °C (with darkening); $CH_2CH_2C_6H_5$, 110–112 °C (with darkening); $CH(CH_3)C_6H_5$, 79–80 °C (with darkening). ^1H NMR: $(\eta^5\text{-}C_5H_5)W(CO)_3CH_2C_6H_5(CDCl_3)$, δ 7.12 (m, 5 H, C_6H_5), 5.26 (s, 5 H, C_5H_5), 2.96 δ (s, 2 H, CH_2); $(\eta^5\text{-}C_5H_5)W(CO)_3CH_2CH_2C_6H_5(\text{acetone-}d_6)$, δ 7.20 (s, 5 H, C_6H_5), 5.69 (s, 5

---

[16] Iler, R. K. "The Chemistry of Silica"; Wiley: New York, 1979. Low, M. J. D.; Parrodi, G. A. *Spectrosc. Lett.* **1978**, *11*, 581.

[17] Robbins, J. L.; Wrighton, M. S. *Inorg. Chem.* **1981**, *20*, 1133.

[18] Kinney, J. B.; Staley, R. H., to be submitted for publication.

H, C_5H_5), 2.90–2.71, 1.84–1.64 (m, 4 H, CH_2CH_2); (η^5-C_5H_5)W-$(CO)_3CH(CH_3)C_6H_5$(acetone-d_6), 7.32–6.94 (m, 5 H, C_6H_5), 5.44 (s, 5 H, C_5H_5), 3.81 (q, J = 7.3 Hz, 1 H, CH), 1.87 (d, J = 7.3 Hz, 3 H, CH_3).

Irradiations. Two General Electric blacklight bulbs (355 ± 20 nm, $\sim 2 \times 10^{-6}$ einstein/min) were used for synthetic purposes. Generally, photolysis experiments involving surface-confined species employed a Hanovia 450-W medium-pressure Hg lamp or a Bausch and Lomb SP200 200 W high-pressure Hg lamp both of which were equipped with a Pyrex filter and 10-cm water filter to suppress IR emissions. Quantum yields at 366 nm were measured in a merry-go-round[19] by using $\sim 10^{-3}$ M (η^5-$C_5R'_5$)M-$(CO)_3R$ with the appropriate ligand concentration. Three-milliliter samples in 13 × 100 mm test tubes were freeze–pump–thaw degassed ($<10^{-5}$ torr, three cycles) and hermetically sealed prior to irradiation. The light source was a 550-W medium-pressure mercury lamp (Hanovia) equipped with Corning glass filters to isolate the 366-nm Hg emission. Ferrioxalate actinometry[20] was used to determine light intensity, typically $\sim 10^{-7}$ einstein/min.

Low-Temperature UV-vis Spectra. Deoxygenated methylcyclohexane solutions of (η^5-C_5H_5)$W(CO)_3R$ ($\sim 10^{-3}$ M) in a 1-cm path-length quartz cell held in a large copper holder were immersed in liquid N_2 contained in a Dewar flask equipped with quartz flats as windows. To take a UV–vis spectrum the level of liquid N_2 was lowered to just below the optical path of the spectrometer making sure, however, that the copper holder was immersed in liquid N_2 at all times. Both cell and holder were kept immersed in liquid N_2 during irradiation with the high-pressure Hg lamp or the beam expanded output ($\sim$5 mW) from an Aerotech, Inc. Model LS5P He–Ne laser operated at 632.8 nm.

Low-Temperature Infrared Spectra. Deoxygenated methylcyclohexane solutions of (η^5-C_5H_5)$W(CO)_3R$ (10^{-2} M) or Nujol mulls of surface-supported species were placed in a 0.1-mm path-length low-temperature IR cell (Precision Cells, Inc. Model P/N 21.000) equipped with CsCl windows. This cell was mounted in the outer holder equipped with CaF_2 or NaCl windows and cooled to 77 K by using liquid N_2 as coolant. Infrared spectra were obtained by using the FTIR at 2- or 4-cm^{-1} resolution.

Synthesis of [SiO_2]–$SiMe_2$–(η^5-C_5H_4)$W(CO)_3R$ (R = Cl, CH_3, C_2H_5). To a suspension of 10 g of dry SiO_2 (corresponding to approximately 27 mmol of free hydroxyl groups) in 200 mL of toluene was added 4.3 mL of freshly distilled pyridine and 8.6 g of $ClSiMe_2C_5H_5$, obtained by using literature procedures.[21] The mixture was refluxed for 24 h and then filtered under vacuum on a medium-fritted glass filter; the derivatized SiO_2 was then washed with 300 mL of methanol to remove pyridinium hydrochloride and with 200 mL of THF and finally dried for 6 h under vacuum. To 1.15 g of the resulting derivatized SiO_2 suspended in $\sim$50 mL of THF was added 4 mL of n-BuLi (2.3 M) and the mixture was refluxed overnight; 3.3 g of $W(CO)_6$ was dissolved in the suspension and further refluxed for 1 day. The mixture was allowed to cool and reacted for 18 h with 14 mmol of alkyl iodide (CH_3I or C_2H_5I) as a stirred suspension at room temperature. The derivatized SiO_2 was finally filtered through a fritted glass filter, washed liberally with THF and hexane, and then dried overnight under vacuum, giving a yellow, fluffy powder for both alkyl substituents.

For R = Cl, 1.5 g of SiO_2 derivatized with $ClSiMe_2C_5H_5$ as described above was suspended in $\sim$80 mL of dry THF, and a solution of 4×10^{-3} mol of isopropyl Grignard reagent in THF was added in one portion, and the mixture was allowed to stir at room temperature for 2 h. A 1.4-g sample of $W(CO)_6$ was added and the solution refluxed overnight. The mixture was then reacted with 0.32 g of NH_4Cl, stirred for 6 h, filtered through a fritted glass filter, and washed liberally with CH_2Cl_2, THF, and isooctane; the resulting yellowish powder was finally dried for 6 h under vacuum.

Synthesis of [P]–$C_6H_4CH_2$–(η^5-C_5H_4)$W(CO)_3CH_3$. A 5-g sample of chloromethylated polystyrene (also known as Merrifield resin[22]) was suspended in 150 mL of dry THF, and 1.5 g of $Na(C_5H_5)$·DME was dissolved in the mixture which was allowed to reflux for 2 days. The polymer was then separated by using a fritted glass filter and washed with two 250-mL portions of CH_3OH and THF. The derivatized polymer was then dried for 2 days under vacuum. A 3.3-g sample of the above material was suspended in 150 mL of THF; 0.6 mL of 2.3 M n-BuLi was then syringed into the mixture; and the solution was stirred for 2 days at room temperature. A 1.06-g sample of $W(CO)_6$ was added and the mixture refluxed for 16 h. Finally, the surface-confined anion was neutralized with 4 mmol of freshly distilled CH_3I followed by overnight refluxing. The deep yellow polymer was then filtered, washed liberally with toluene, THF, and hexane, and dried overnight under vacuum.

Synthesis of (η^5-C_5H_5)$W(CO)_3$(η^1-$CH_2C_6H_4$–[P]). A 0.18-g sample of $Na[C_5H_5]$·DME and 0.35 g of $W(CO)_6$ were dissolved in $\sim$80 mL of THF, and the solution was refluxed for 3 days. A 3-g sample of chloromethylated polystyrene was added to the solution and the mixture allowed to stir for 24 h at room temperature. The polymer was then filtered under vacuum and washed with 100-mL portions of MeOH, Et_2O, hexane, and finally THF, yielding a bright yellow compound, which was allowed to dry overnight under vacuum.

Results

a. Synthesis and Characterization of Surface-Supported Species. Functionalization of [SiO_2]– and [P]–$C_6H_4CH_2Cl$ follows closely the established pathways used to derivatize such surfaces. In the case of [SiO_2] these are surface OH groups that react with Si–Cl or Si–OR, and the [P]–$C_6H_4CH_2Cl$ bears a benzyl chloride that can be reacted with anions to displace the chloride. The overall synthetic procedures used to prepare the various complexes anchored on [SiO_2]– are represented by eq 3–8, and the

$$[SiO_2]\text{–}OH + ClSiMe_2C_5H_5 \rightarrow [SiO_2]\text{–}SiMe_2C_5H_5 + HCl \quad (3)$$

$$[SiO_2]\text{–}SiMe_2C_5H_5 + n\text{-BuLi} \rightarrow [SiO_2]\text{–}SiMe_2C_5H_4^{-}Li^{+} + n\text{-BuH} \quad (4)$$

$$[SiO_2]\text{–}SiMe_2C_5H_4^{-}Li^{+} + W(CO)_6 \rightarrow [SiO_2]\text{–}SiMe_2\text{–}(\eta^5\text{-}C_5H_4)W(CO)_3^{-}Li^{+} + 3CO \quad (5)$$

$$[SiO_2]\text{–}SiMe_2\text{–}(\eta^5\text{-}C_5H_4)W(CO)_3^{-}Li^{+} + CH_3I \rightarrow [SiO_2]\text{–}SiMe_2\text{–}(\eta^5\text{-}C_5H_4)W(CO)_3CH_3 + LiI \quad (6)$$

$$[SiO_2]\text{–}SiMe_2\text{–}(\eta^5\text{-}C_5H_4)W(CO)_3^{-}Li^{+} + C_2H_5I \rightarrow [SiO_2]\text{–}SiMe_2\text{–}(\eta^5\text{-}C_5H_4)W(CO)_3C_2H_5 + LiI \quad (7)$$

$$[SiO_2]\text{–}SiMe_2\text{–}(\eta^5\text{-}C_5H_4)W(CO)_3^{-}Li^{+} \xrightarrow{H^+} \xrightarrow{RCl} [SiO_2]\text{–}SiMe_2\text{–}(\eta^5\text{-}C_5H_4)W(CO)_3Cl \quad (8)$$

details are given in the Experimental Section. At each step in the synthesis of [SiO_2]–$SiMe_2$–(η^5-C_5H_4)$W(CO)_3R$ there is the possibility of both low yield and side reactions. However, FTIR spectra of the functionalized powders in KBr disks or as Nujol mulls show the metal carbonyl region to be free of metal carbonyl impurities. For example, Figures 1 and 2 illustrate the excellent IR spectra that can be obtained for the surface-confined species showing two strong IR absorptions, in position and relative intensity, that confirm the presence of the bound organometallic species. Table I lists IR data for surface species and appropriate pure substances. In every case, the IR spectrum for the surface-bound species accords well with the model complex. We conclude that anchoring the complexes does not significantly alter their geometrical or electronic

---

(19) Moses, F. G.; Liu, R. S. H.; Monroe, B. M. *Mol. Photochem.* **1969**, *1*, 245.

(20) Hatchard, C. G.; Parker, C. A. *Proc. R. Soc. London, Ser. A* **1956**, 235.

(21) Schaaf, R. L.; Kan, P. T.; Lenks, C. T.; Deck, E. P. *J. Org. Chem.* **1960**, *25*, 1986.

(22) Merrifield, R. B. *Fed. Proc., Fed. Am. Soc. Exp. Biol.* **1962**, *21*, 412. Merrifield, R. B. *Science (Washington, D.C.)* **1965**, *150*, 178.

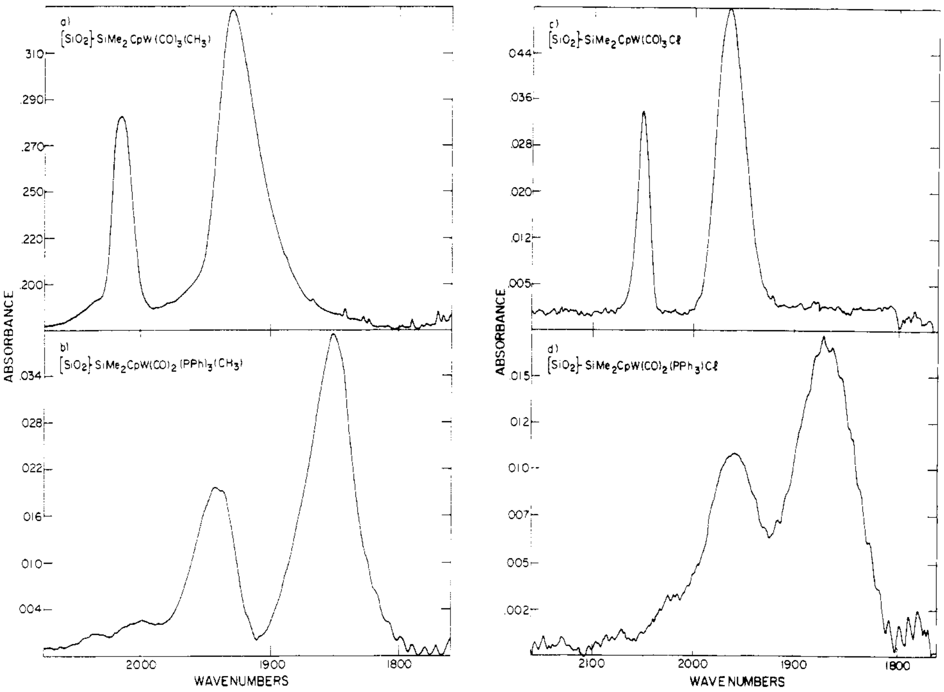

Figure 1. Infrared spectra in the carbonyl stretching region of SiO_2-supported species at 300 K as KBr pellets: (a) $[SiO_2]–SiMe_2–(\eta^5\text{-}C_5H_4)W(CO)_3CH_3$ synthesized as described in the text; (b) $[SiO_2]–SiMe_2–(\eta^5\text{-}C_5H_5)W(CO)_2(PPh_3)CH_3$ formed upon irradiation of the sample suspended in THF containing 0.1 M PPh_3; (c) $[SiO_2]–SiMe_2–(\eta^5\text{-}C_5H_4)W(CO)_3Cl$ prepared as described in the text; (d) $[SiO_2]–SiMe_2–(\eta^5\text{-}C_5H_4)W(CO)_2(PPh_3)Cl$ formed upon irradiation of the sample suspended in THF solution containing 0.1 M PPh_3.

structure, since the CO stretching region of metal carbonyls is quite sensitive to both.

Consistent with the conclusion from the IR spectra, the UV–vis absorption of $[SiO_2]–SiMe_2–(\eta^5\text{-}C_5H_4)W(CO)_3R$ accords satisfactorily with the appropriate $(\eta^5\text{-}C_5H_5)W(CO)_3R$ model, Table I. The UV–vis data for the surface-confined species were obtained by using photoacoustic spectroscopy. The apparent discrepencies in band positions in the models vs. the surface species are likely due to the fact that the absorption maxima are generally just shoulders and for the $[SiO_2]$-bound systems there is background signal in the photoacoustic spectra beginning at ~330 nm from the $[SiO_2]$–.

The presence of the strong IR bands in the CO stretching region and the elemental analyses (vide infra) do confirm that the metal carbonyls are on the surface. Further, the metal carbonyls are covalently anchored; the homogeneous models show no persistent attachment to the $[SiO_2]$–. However, as indicated above, there may be other functional groups on the surface such as $[SiO_2]–OR$ (R = CH_3, C_2H_5), from chemistry represented by eq 9 and 10,

$$[SiO_2]–OH + n\text{-}BuLi \rightarrow [SiO_2]–O^-Li^+ + n\text{-}BuH \qquad (9)$$

$$[SiO_2]–O^-Li^+ + RI \rightarrow [SiO_2]–OR + LiI \qquad (10)$$

or unreacted $[SiO_2]–SiMe_2C_5H_5$. The importance of these other functional groups is likely to be low in the present systems, since the metal carbonyl can be selectively photoexcited owing to optical absorption differences. The spectra in the C–H stretching region of $[SiO_2]–SiMe_2C_5H_5$ and $[SiO_2]–SiMe_2–(\eta^5\text{-}C_5H_4)W(CO)_3Cl$ are shown in Figure 3; the spectra accord well with that in the same region for $ClSiMe_2C_5H_5$. These data do not unambiguously rule out significant coverages of $[SiO_2]–OR$, but it appears that the desired material dominates the spectra. However, the elemental analyses, Table II, do not always accord well with the expected ratio of elements. This is clearly a problem common to all forms of surface modification. Purification procedures employed for solution substances cannot be applied to such systems.

The $[P]–C_6H_4CH_2–(\eta^5\text{-}C_5H_4)W(CO)_3CH_3$ species were prepared according to eq 11–14, and the $[P]–C_6H_4CH_2W(CO)_3(\eta^5\text{-}C_5H_5)$ was prepared according to eq 15 and 16.

$$[P]–C_6H_4CH_2Cl + Na[C_5H_5] \rightarrow [P]–C_6H_4CH_2C_5H_5 + NaCl \qquad (11)$$

$$[P]–C_6H_4CH_2C_5H_5 + n\text{-}BuLi \rightarrow [P]–C_6H_4CH_2C_5H_4^-Li^+ + n\text{-}BuH \qquad (12)$$

$$[P]–C_6H_4CH_2C_5H_4^-Li^+ + W(CO)_6 \rightarrow [P]–C_6H_4CH_2–(\eta^5\text{-}C_5H_4)W(CO)_3^-Li^+ + 3CO \qquad (13)$$

$$[P]–C_6H_4CH_2–(\eta^5\text{-}C_5H_4)W(CO)_3^-Li^+ + CH_3I \rightarrow [P]–C_6H_5CH_2–(\eta^5\text{-}C_5H_4)W(CO)_3CH_3 + LiI \qquad (14)$$

$$W(CO)_6 + Na[C_5H_5] \rightarrow Na[(\eta^5\text{-}C_5H_5)W(CO)_3] + 3CO \qquad (15)$$

$$[P]–C_6H_4CH_2Cl + Na[(\eta^5\text{-}C_5H_5)W(CO)_3] \rightarrow (\eta^5\text{-}C_5H_5)W(CO)_3(\eta^1\text{-}CH_2C_6H_4)–[P] + NaCl \qquad (16)$$

As for the $[SiO_2]$– systems, the $[P]–C_6H_4CH_2$– systems can be characterized by IR and UV–vis spectra to confirm the presence of the metal carbonyl (Table I). However, the IR spectra, even in the unique CO stretching region, are complicated by overtone absorptions from the polymer itself. Figure 4 illustrates the situation and shows that partial photoreaction, coupled with the ability to manipulate the spectra (subtract initial from final), can reveal the positions of the CO stretching frequencies for the surface-bound organometallic species. Simple subtraction of a spectrum of the $[P]–C_6H_4CH_2Cl$ from the $[P]–C_6H_4CH_2$– derivative is doable, but the presence of the derivative can cause subtle changes in polymer structure that make this procedure somewhat unreliable.

Coverage of the surface-confined metal carbonyls has been determined by IR measurements in the following way. Model compounds are measured in KBr disks prepared in as reproducible a fashion as possible. The absolute absorbance of the "standard" in the CO stretching region is thus established. The $[SiO_2]$– and $[P]–C_6H_4CH_2$– sys-

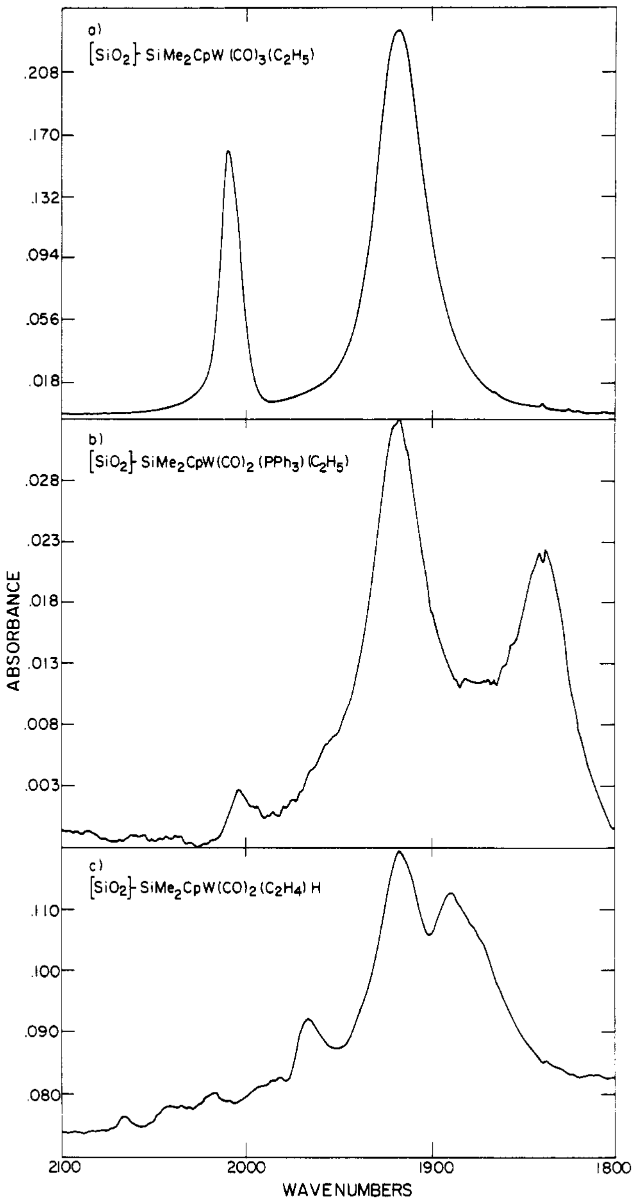

Figure 2. Infrared spectra in the carbonyl stretching region of [SiO_2]-supported species: (a) [SiO_2]–$SiMe_2$–(η^5-C_5H_4)$W(CO)_3C_2H_5$ prepared as described in the text; (b) [SiO_2]–$SiMe_2$–(η^5-C_5H_4)-$W(CO)_2(PPh_3)C_2H_5$ formed upon irradiation of the sample suspended in THF solution containing 0.5 M PPh_3; (c) [SiO_2]–$SiMe_2$–(η^5-C_5H_4)$W(CO)_2(H)(C_2H_4)$ formed upon irradiation of a sample suspended in THF with no deliberately added ligand.

tems are then measured in the same way to determine absorbance for a known mass of the derivatized power in a standard KBr disk. The measurement thus gives the average coverage of metal carbonyl on the surface. An independent method for determining coverages of surface species is elemental analysis. The amount of W, unique to the surface-supported species, is determined and used to calculate surface coverage. Data for coverage determinations both by infrared analysis and elemental analysis are given in Table II. Also included are coverages for [SiO_2]– supported species in units of mol/cm^2 where a monolayer corresponds to approximately 10^{-10} mol/cm^2. The surface area used is 400 m^2/g and corresponds to the reported surface area of the underivatized [SiO_2]–. Further, a mean separation distance for W centers is also calculated on the basis of this value where $\bar{d} \simeq 1/(N_{AV}C)^{1/2}$, where N_{AV} is Avogadro's number and C is the coverage in mol/cm^2. The value of $\bar{d}$ is generally in the range ~10–20 Å.

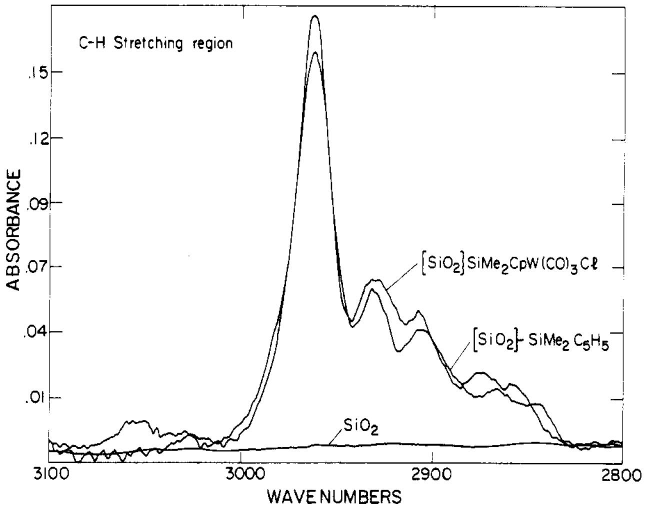

Figure 3. Infrared spectra in the C–H stretching region of [SiO_2]-supported species taken as KBr pellets at 300 K.

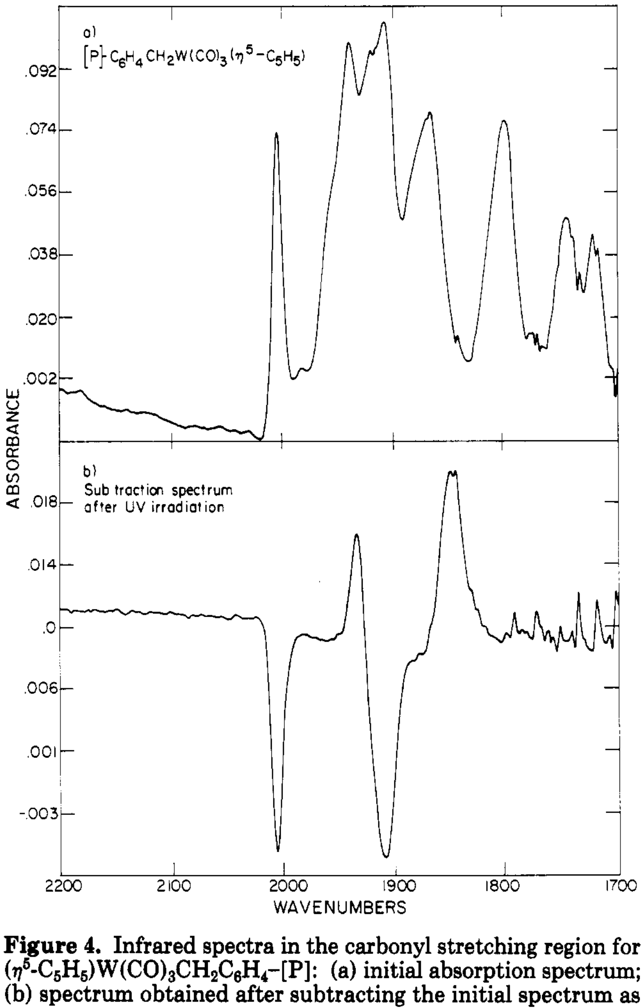

Figure 4. Infrared spectra in the carbonyl stretching region for (η^5-C_5H_5)$W(CO)_3CH_2C_6H_4$–[P]: (a) initial absorption spectrum; (b) spectrum obtained after subtracting the initial spectrum as shown in (a) from a spectrum obtained after irradiation of surface-supported species. This difference spectrum shows the disappearance of (η^5-C_5H_5)$W(CO)_3$(η^1-$CH_2C_6H_4$–[P]) as negative peaks at 2007 and 1915 cm^{-1} and the appearance of (η^5-C_5H_5)W-$(CO)_2$(η^3-$CH_2C_6H_4$–[P]) as positive peaks at 1934 and 1847 cm^{-1}.

b. Photochemistry of Surface Species. Dissociative loss of CO occurs as the primary result of photoexcitation of (η^5-C_5H_5)$W(CO)_3R$ in solution.[14] This reaction is efficient ($\Phi_{366} > 0.1$, Table III) and generates a reactive 16-valence-electron species (η^5-C_5H_5)$W(CO)_2R$ which can undergo subsequent thermal reactions such as ligand addition, β-hydrogen transfer and η^1- → η^3-allyl conversion

Table II. Surface Coverages for Surface-Confined Molecules from Infrared Spectroscopy and Elemental Analyses

complex	elemental anal. element (wt % found)	coverage,[a] mol/g (mol/cm²) elemental anal.	coverage,[a] mol/g (mol/cm²) IR anal.	$\bar{d}$,[b] Å elemental anal.	$\bar{d}$,[b] Å IR anal.
$[SiO_2]$–$SiMe_2$–(η^5-C_5H_4)$W(CO)_3CH_3$	W (5.5), C (6.8)	3.0×10^{-4} (7.5×10^{-11})	6.2×10^{-4} (16×10^{-11})	15	10
$[SiO_2]$–$SiMe_2$–(η^5-C_5H_4)$W(CO)_3C_2H_5$	W (7.7), C (5.7)	4.2×10^{-4} (10×10^{-11})	1.8×10^{-4} (4.4×10^{-11})	13	19
$[SiO_2]$–$SiMe_2$–(η^5-C_5H_4)$W(CO)_3Cl$	W (7.8), C (7.1), Cl (1.9)	4.3×10^{-4} (10×10^{-11})	0.2×10^{-4} (0.5×10^{-11})	13	56
[P]–$C_6H_4CH_2$–(η^5-C_5H_4)$W(CO)_3CH_3$	W (4.4), Cl (0.3), O (3.2)	2.4×10^{-4}	1.1×10^{-4}		
[P]–$C_6H_4CH_2$–(η^5-C_5H_4)$W(CO)_3C_2H_5$	W (3.6), Cl (1.1), O (5.2)	2.0×10^{-4}	0.6×10^{-4}		
(η^5-C_5H_4)$W(CO)_3CH_2C_6H_4$–[P]	W (0.59), Cl (1.0), O (1.3)	0.3×10^{-4}	0.8×10^{-4}		

[a] Surface density of W species based on elemental analysis for tungsten or on infrared analysis SiO_2 surface area was taken 400 m²/g. [b] Approximate smallest mean distance between W centers given by $(N_{AV}C)^{-1/2}$, where N_{AV} is Avogadro's number and C is the coverage.

Table III. Quantum Yields for the Disappearance of (η^5-C_5H_5)$W(CO)_3R$ at 366 nm

compd	$\Phi \pm 10\%$[a]
(η^5-C_5H_5)$W(CO)_3CH_2C_6H_5$	0.31
(η^5-C_5H_5)$W(CO)_3CH_2CH_2C_6H_5$	0.35
(η^5-C_5H_5)$W(CO)_3CH(CH_3)C_6H_5$	0.30
(η^5-C_5H_5)$W(CO)_3C_2H_5$	0.34
(η^5-C_5H_5)$W(CO)_3CH_3$	0.38[b]
(η^5-C_5H_5)$W(CO)_3Cl$	0.38[c]

[a] Φ's are for ~1 mM complex dissolved in isooctane for <10% conversion. For the compounds where R = η^1-$CH_2C_6H_5$ and η^1-$CH(CH_3)C_6H_5$ the only product observed is η^3-$CH_2C_6H_5$ and η^3-$CH(CH_3)C_6H_5$, respectively. For R = η^1-$CH_2CH_2C_6H_5$ both (η^5-C_5H_5)$W(CO)_2$(H)(styrene) and (η^5-C_5H_5)$W(CO)_2$(η^3-$CH(CH_3)C_6H_5$) are observed. For R = C_2H_5, (η^5-C_5H_5)$W(CO)_2(H)(C_2H_4)$ is the only observed product. [b] Quantum yield for disappearance of 10 mM (η^5-C_5H_5)$W(CO)_3CH_3$ in the presence of 0.5 M PPh_3 in toluene. (η^5-C_5H_5)$W(CO)_2(PPh_3)CH_3$ is the only observed product. [c] Quantum yield for the appearance of *cis*-(η^5-C_5H_5)$W(CO)_2(PPh_3)Cl$ when 1 mM (η^5-C_5H_5)$W(CO)_3Cl$ in benzene solution containing 5 mM PPh_3 is irradiated. Data taken from: Alway, D. G.; Barnett, K. W. *Inorg. Chem.* **1980**, *19*, 1533.

(vide infra) all of which reestablish an 18-valence-electron count. Definitive evidence for CO loss as the primary reaction upon photoexcitation is provided by the direct observation of the resulting (η^5-C_5H_5)$W(CO)_2R$ when the irradiation is carried out at sufficiently low temperatures.[14]

Results to be developed below establish dissociative loss of CO to be as the primary result of excitation of surface-supported (η^5-C_5H_5)$W(CO)_3R$. Figures 1 and 2 show the infrared spectra of the substitution products obtained upon irradiating $[SiO_2]$–$SiMe_2$–(η^5-C_5H_4)$W(CO)_3R$ as a suspension in THF containing 0.1–0.5 M PPh_3. The infrared spectra show clean conversion to the corresponding $[SiO_2]$–$SiMe_2$–(η^5-C_5H_4)$W(CO)_2(PPh_3)R$ based on comparison to the spectra of analogous solution species (Table I). Irradiation of $[SiO_2]$–$SiMe_2$–(η^5-C_5H_4)$W(CO)_3C_2H_5$ in the absence of ligand at 300 K as a suspension results in loss of CO followed by β-hydrogen transfer, eq 17 and 18.

$$[SiO_2]\text{–}SiMe_2\text{–}(\eta^5\text{-}C_5H_4)W(CO)_3R \underset{\Delta}{\overset{h\nu}{\rightleftharpoons}} CO + [SiO_2]\text{–}SiMe_2\text{–}(\eta^5\text{-}C_5H_4)W(CO)_2R \quad (17)$$

$$[SiO_2]\text{–}SiMe_2\text{–}(\eta^5\text{-}C_5H_4)W(CO)_2C_2H_5 \xrightarrow{\Delta} [SiO_2]\text{–}SiMe_2\text{–}(\eta^5\text{-}C_5H_4)W(CO)_2(C_2H_4)H \quad (18)$$

The infrared spectral changes associated with the 300 K irradiation of $[SiO_2]$–$SiMe_2$–(η^5-C_5H_4)$W(CO)_3C_2H_5$ in the absence of PPh_3, Figure 2c, show features that could be attributable to $[SiO_2]$–$SiMe_2$–(η^5-C_5H_4)$W(CO)_2(H)(C_2H_4)$, ~1892 and 1969 cm⁻¹, but additionally there is a broad, rather intense feature at ~1920 cm⁻¹ that is not found upon irradiating the analogous solution species (η^5-C_5H_5)$W(CO)_3C_2H_5$. This feature could be due to a surface-confined metal carbonyl arising from an interaction of the photogenerated 16-valence-electron species with the surface. In any event, the spectrum is not as unambiguous as for the substitution by PPh_3, Figures 1 and 2b. However, chemical changes from irradiation of the surface-bound ethyl complex do occur that are not found for the analogous surface-bound methyl complex. Presumably, the photoejection of CO into the solution is essentially completely reversible in the case of R = CH_3 whereas β-hydrogen transfer competes with back-reaction when R = C_2H_5.

Irradiation of $[SiO_2]$–$SiMe_2$–(η^5-C_5H_4)$W(CO)_3R$ (R = CH_3, C_2H_5) as a Nujol suspension at 77 K while monitoring

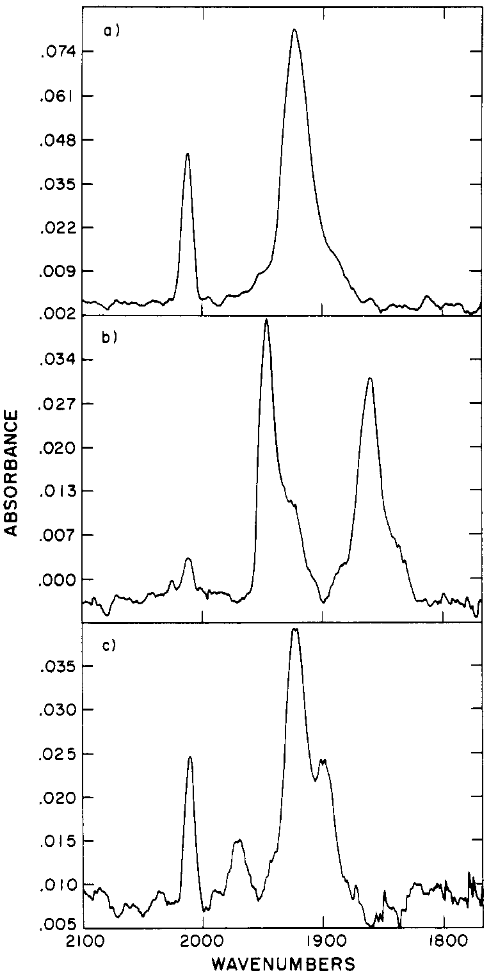

Figure 5. Infrared spectra in the carbonyl stretching region of $[SiO_2]$-supported species taken as Nujol mulls: (a) $[SiO_2]$–$SiMe_2$–$(\eta^5\text{-}C_5H_4)W(CO)_3C_2H_5$ at 77 K; (b) after irradiation of the sample shown in a at 77 K showing the formation of $[SiO_2]$–$SiMe_2$–$(\eta^5\text{-}C_5H_4)W(CO)_2C_2H_5$; (c) after warming the sample shown in b to 300 K showing regeneration of starting material and β-hydrogen transfer to form $[SiO_2]$–$SiMe_2$–$(\eta^5\text{-}C_5H_4)W(CO)_2(H)(C_2H_4)$.

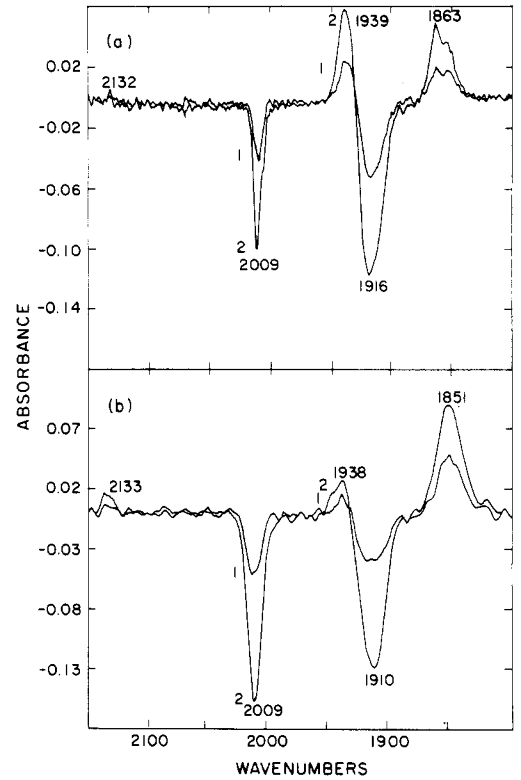

Figure 6. Difference infrared spectra showing reactions of solution and polymer supported $(\eta^5\text{-}C_5H_5)W(CO)_3(\eta^1\text{-}CH_2C_6H_5)$ at 77 K: (a) the initial spectrum of a ~1 mM solution of $(\eta^5\text{-}C_5H_5)W(CO)_3(\eta^1\text{-}CH_2C_6H_5)$ in methylcyclohexane at 77 K is subtracted from subsequent spectra obtained after 5- (trace 1) and 30-min (trace 2) 355-nm irradiation; (b) the initial spectrum of a Nujol mull (~0.1-mm path length) of $(\eta^5\text{-}C_5H_5)W(CO)_3$-$(\eta^1\text{-}CH_2C_6H_4$–[P]) at 77 K is subtracted from subsequent spectra obtained after 5 (trace 1) and 20 s (trace 2) irradiation with a water-filtered high-pressure Hg lamp.

by infrared spectroscopy provides direct support for the dissociative loss of CO following photoexcitation, Figure 5 and Table I. As for homogeneous solution analogues, the irradiation at 77 K yields decline of the two starting material absorptions and the growth of two new metal carbonyl features at ~1850 and ~1950 cm^{-1}. Additionally, a feature at 2133 cm^{-1} grows in that can be attributed to the photoejected CO. As shown in Figure 5b, the spectral changes are substantial and clean and nearly perfectly accord with the homogeneous analog.[14] Warming the 77 K suspension after irradiation yields further infrared spectral changes for the surface-bound ethyl complex, Figure 5c, accompanied by significant regeneration of $[SiO_2]$–$SiMe_2$–$(\eta^5\text{-}C_5H_4)W(CO)_3C_2H_5$. For the surface-bound methyl species only regeneration of starting material occurs upon warming the 77 K suspension. The further spectral changes upon warming the ethyl complex, Figure 5c, evidence the generation of $[SiO_2]$–$SiMe_2$–$(\eta^5\text{-}C_5H_4)W(CO)_2(H)(C_2H_4)$. Thus, data represented by Figure 5 directly support the conclusion that reactions according to eq 17 and 18 occur upon irradiation of the surface-bound alkyl complexes. The methyl complex has no β-hydrogens and only back-reacts with CO upon warm-up at the 16-valence-electron stage.

Irradiation of either surface-confined or solution $(\eta^5\text{-}C_5H_5)W(CO)_3(\eta^1\text{-}CH_2C_6H_5)$ results in formation of $(\eta^5\text{-}C_5H_5)W(CO)_2(\eta^3\text{-}CH_2C_6H_5)$. Figures 6 and 7 show difference infrared spectra in the carbonyl stretching region obtained upon irradiation of $(\eta^5\text{-}C_5H_5)W(CO)_3(\eta^1\text{-}CH_2C_6H_4$–[P]) and solution $(\eta^5\text{-}C_5H_5)W(CO)_3(\eta^1\text{-}CH_2C_6H_5)$ and $(\eta^5\text{-}C_5H_5)W(CO)_3(\eta^1\text{-}CH(CH_3)C_6H_5)$ at 77 K. Since the infrared stretching frequencies for $(\eta^5\text{-}C_5H_5)W(CO)_2R$ and $(\eta^5\text{-}C_5H_5)W(CO)_2(\eta^3$-benzyl) are not well separated (Table I), it is not possible to distinguish on the basis of the infrared spectrum alone whether an η^1 to η^3 conversion takes place at 77 K or whether the 77 K spectral changes simply reflect formation of the presumed 16-valence-electron intermediate. However, the optical spectra for the η^3-benzyl and the 16-valence-electron species at 77 K should be quite different.[14] Figure 8 shows the UV–vis spectral changes that occur upon irradiation of two benzyl species in a methylcyclohexane glass at 77 K. The spectral changes observed for R = $CH_2C_6H_5$ and $CH(CH_3)C_6H_5$ at 77 K are inconsistent with the formation of a long-lived 16-valence-electron species that should have an absorption maximum in the 550–620-nm range.[14] When the irradiated sample was warmed from 77 to 300 K, the UV–vis spectra change only modestly and infrared and UV–vis data unequivocally establish that the $(\eta^5\text{-}C_5H_5)W(CO)_2(\eta^3$-benzyl) species is present.[23] Thus, the lack of a low-energy visible absorption band at 77 K upon irradiation as can be observed for $(\eta^5\text{-}C_5H_5)W(CO)_2R$ (R = CH_3, C_2H_5)[14] shows that the absorption bands in the infrared, Figures 6 and 7, after irradiation of the η^1-benzyl species at 77 K are due

---

[23] Faller, J. W.; Chen, C.; Mattina, M. J.; Jakubowski, A. *J. Organomet. Chem.* **1973**, *52*, 361.

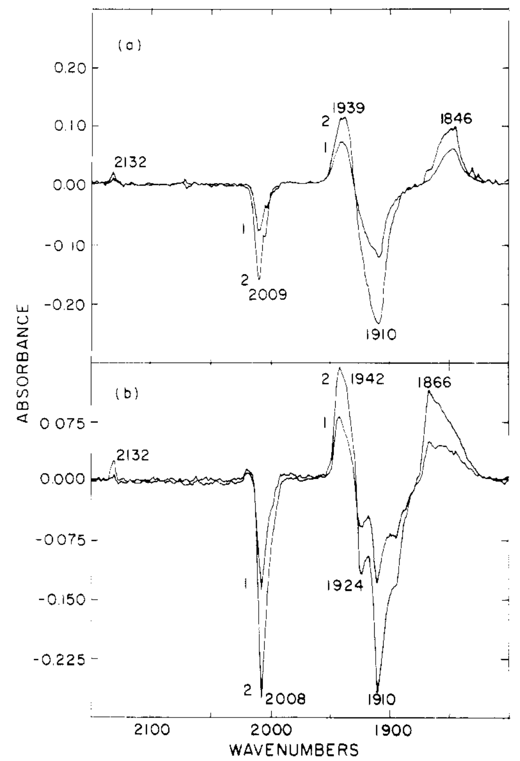

Figure 7. Difference infrared spectra showing reactions of $(\eta^5\text{-}C_5H_5)W(CO)_3R$ in methylcyclohexane glass at 77 K. (a) The initial spectrum of a ~1 mM solution of $(\eta^5\text{-}C_5H_5)W(CO)_3CH_2CH_2C_6H_5$ is subtracted from subsequent spectra obtained after 5- (trace 1) and 20-min (trace 2) irradiation with 355-nm light. Warming the resulting solution to 300 K results in infrared changes consistent with the disappearance of the product formed at 77 K and formation of *trans*-$(\eta^5\text{-}C_5H_5)W(CO)_2(H)$(styrene) and $(\eta^5\text{-}C_5H_5)W(CO)_2(\eta^3\text{-}CH(CH_3)C_6H_5)$. (b) The initial spectrum of a ~5 mM solution of $(\eta^5\text{-}C_5H_5)W(CO)_3(\eta^1\text{-}CH(CH_3)C_6H_5)$ is subtracted from subsequent spectra obtained after 5- (trace 1) and 20-s (trace 2) irradiation with a water-filtered high-pressure Hg lamp. Warming the resulting solution to 300 K does not cause significant spectral changes.

to the η^3-benzyl species and not a 16-valence-electron species. We conclude that the conversion of an η^1- to η^3-benzyl, eq 19, occurs rapidly at 77 K (complete as soon

$$(\eta^5\text{-}C_5H_5)W(CO)_2(\eta^1\text{-}CH_2C_6H_5) \xrightarrow{\Delta} (\eta^5\text{-}C_5H_5)W(CO)_2(\eta^3\text{-}CH_2C_6H_5) \quad (19)$$

as an FTIR spectrum can be taken, ~60 s). With the assumption of an Arrhenius factor of 10^{14} s^{-1}, an upper limit of 6 kcal/mol can be set on the activation energy for this unimolecular thermal process.

The $(\eta^5\text{-}C_5H_5)W(CO)_3CH_2CH_2C_6H_5$ complex can be viewed as an η^3-benzyl precursor which requires isomerization to $\eta^1\text{-}CH(CH_3)C_6H_5$ before η^3 coordination can occur. Infrared spectral changes accompanying irradiation at 77 K of $(\eta^5\text{-}C_5H_5)W(CO)_3CH_2CH_2C_6H_5$, Figure 7a, suggest that $(\eta^5\text{-}C_5H_5)W(CO)_2CH_2CH_2C_6H_5$ is the principal product. The corresponding UV–vis spectral changes, Figure 8b, clearly differ from those for η^1-benzyl complexes. A low-energy visible absorption at ~565 nm is found which is characteristic of coordinatively unsaturated $(\eta^5\text{-}C_5H_5)W(CO)_2R$.[14] This new band decreases upon irradiation at 632.8 nm with a concomitant increase of a shoulder at ~430 nm. This 632.8-nm induced spectral charge has been attributed to the conversion of a fully coordinatively unsaturated species to one where the metal interacts with the β-hydrogen, eq 20 in analogous alkyl complexes. Warming of the irradiated sample results in β-hydrogen transfer, eq 21, as shown by infrared spectroscopy, Table I. The ^{1}H

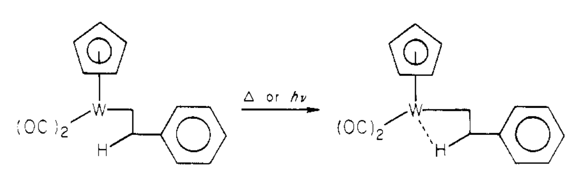

(20)

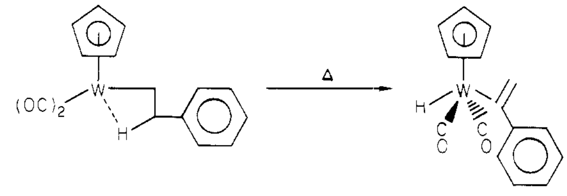

(21)

NMR spectrum shows a characteristic hydride resonance at δ −5.7 upfield from tetramethylsilane, for $(\eta^5\text{-}C_5H_5)W(CO)_2(H)$(styrene). This hydride resonance disappears completely upon addition of CCl_4 and a resonance for $HCCl_3$ appears, characteristic of metal hydrides. The trans arrangement of the carbonyls is assigned on the basis of relative intensities of the carbonyl stretches (1:1.6) which allows a calculation of 103° for the OC–M–CO angle[24] in good agreement with molecular structures of similar compounds obtained by X-ray diffraction.[25] Related complexes have also been determined to have the trans geometry.[14] The *trans*-styrene hydride isomerizes to form $(\eta^5\text{-}C_5H_5)W(CO)_2(\eta^3\text{-}CH(CH_3)C_6H_5)$, eq 22. This reaction

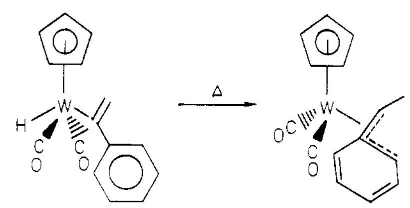

(22)

has been monitored by infrared spectroscopy in the carbonyl region as a function of time and occurs with a first-order rate constant of (1.7 ± 0.2) × 10^{-3} s^{-1} at 298 K. Reaction according to eq 22 goes to completion (>95%). Pure $(\eta^5\text{-}C_5H_5W(CO)_2(\eta^3\text{-}CH(CH_3)C_6H_5)$ does not yield any detectable styrene–hydride at 298 K when dissolved in alkane solvents.

Two additional important qualitative results concerning the photochemistry of surface-confined $(\eta^5\text{-}C_5H_5)W(CO)_2R$ ($R = CH_3$, C_2H_5) should be described. First, the irradiation of $[SiO_2]\text{-}SiMe_2\text{-}(\eta^5\text{-}C_5H_4)W(CO)_3CH_3$ as a powder exposed to a 4/1 Ar/O_2 atmosphere results in rapid reaction. When the surface and gas-phase products, Figure 9, are monitored by FTIR/PAS,[9,18] the chemistry can be seen to involve reaction of O_2 with the surface-confined, photogenerated 16-valence-electron metal carbonyl. The gas-phase products include CO_2, presumably from the oxidation of a bound CO,[9] along with CO and CH_4. No new metal carbonyls are detected as surface products and presumably indicates that the metal-containing product is an oxide as previously reported for surface-confined cobalt tetracarbonyl.[9] The mechanism for CH_4 formation remains to be elucidated, bu the low-temperature photochemistry rules out prompt formation of CH_3 radicals subsequent to photoexcitation. Interfacial gas/solid photochemistry in this and related systems will be detailed elsewhere.

---

(24) Cotton, F. A.; Wilkinson, G. "Advanced Inorganic Chemistry", 4th ed.; Wiley Interscience: New York. The lower energy band is assigned as the asymmetric stretch based on arguments presented in: Cotton, F. A.; Kraihanzel, G. S. *J. Am. Chem. Soc.* **1962**, *84*, 4432.

(25) $(\eta^5\text{-}C_5H_5)Mo(CO)_3C_2H_5$ has a trans OC–Mo–CO angle of 106° based on X-ray diffraction data in: Bennett, M. J.; Mason, R. *Proc. Chem. Soc., London* **1963**, 273.

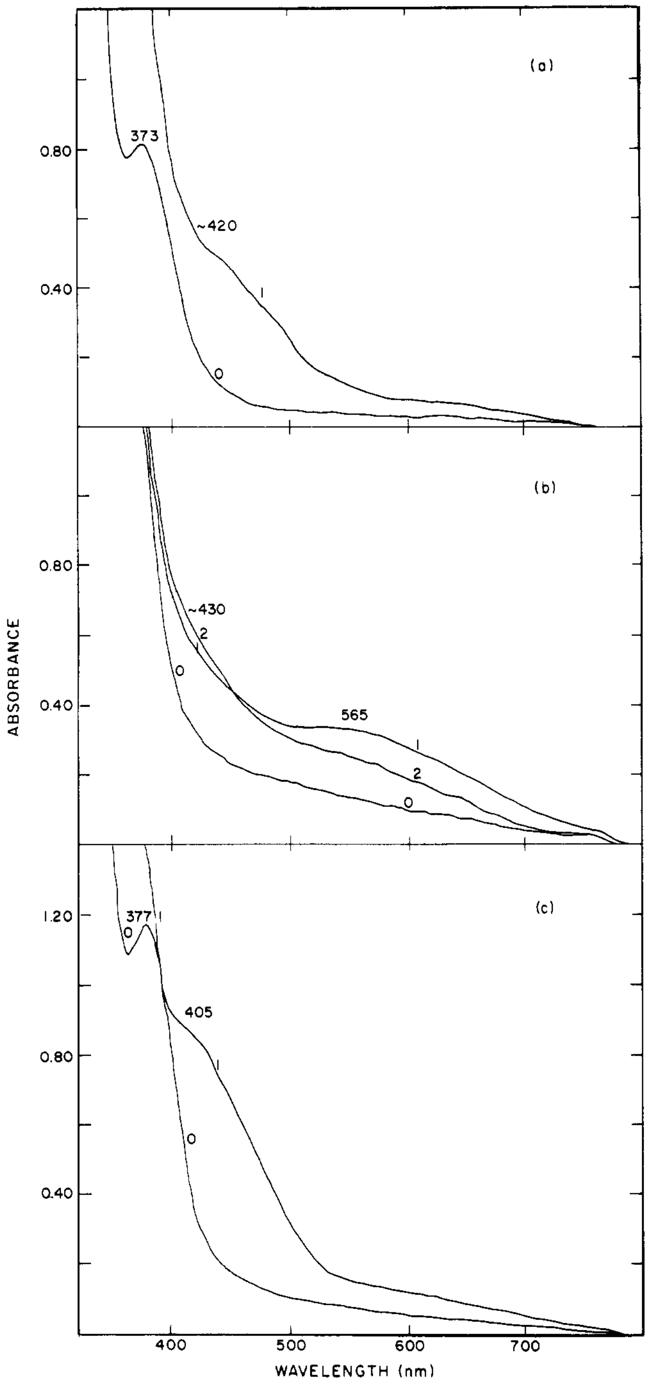

Figure 8. UV-vis spectra of $(\eta^5\text{-}C_5H_5)W(CO)_3R$ at 77 K in methylcyclohexane glass. (a) 6 × 10^{-4} M $(\eta^5\text{-}C_5H_5)W(CO)_3(\eta^1\text{-}CH_2C_6H_5)$ before (scan 0) and after (scan 1) 30-min irradiation with 355-nm light at 77 K. UV-vis of final solution does not change upon warming to 300 K. Infrared analysis of the solution after warming shows ~25% conversion of starting material to the $\eta^3\text{-}CH_2C_6H_5$ species. (b) 8 × 10^{-4} M $(\eta^5\text{-}C_5H_5)W(CO)_3CH_2CH_2C_6H_5$ before (scan 0) and after (scan 1) 30-min irradiation with blacklight at 77 K. Scan 2 shows the results of irradiation of the photoproduct with a 5 mW laser at 632.8 nm. (c) 7 × 10^{-4} M $(\eta^5\text{-}C_5H_5)W(CO)_3(\eta^1\text{-}CH(CH_3)C_6H_5)$ before (scan 0) and after (scan 1) 5-min high-pressure Hg lamp irradiation. UV-vis of the final solution does not change upon warming to 300 K. All spectra are uncorrected for solvent contraction.

The second qualitative result relates to the ability to demonstrate that the surface-confined metal carbonyls are sufficiently well separated so that W–W bonds cannot form. Irradiation of solution $(\eta^5\text{-}C_5H_4)W(CO)_3R$ species invariably leads to some $(\eta^5\text{-}C_5H_5)W_2(CO)_6$ for all situations except very low conversions.[14] The W–W-bonded species result from secondary thermal and photochemical reactions, since W–R homolysis is an unimportant primary photoprocess.[14] Generally, no W–W species are detected after irradiation of any of the surface-confined species. To establish that the surface-bound species can efficiently form W–W-bonded complexes, we have carried out an irradiation of $[SiO_2]\text{–}SiMe_2\text{–}(\eta^5\text{-}C_5H_4)W(CO)_3C_2H_5$ as a THF suspension containing dissolved $(\eta^5\text{-}C_5H_5)W(CO)_3C_2H_5$. Isolation and washing of the derivatized $[SiO_2]$– with THF gives a pink solid having a UV-vis/PAS spectrum nearly identical with that for appropriately diluted $(\eta^5\text{-}C_5H_5)_2W_2(CO)_6$, Figure 10. The infrared spectrum of the derivatized $[SiO_2]$– also accords well with that for $(\eta^5\text{-}C_5H_5)_2W_2(CO)_6$ in the CO stretching region. Solution $(\eta^5\text{-}C_5H_5)_2W_2(CO)_6$ is also formed and does not persistently bind to $[SiO_2]$–. We thus conclude that $[SiO_2]\text{–}SiMe_2\text{–}(\eta^5\text{-}C_5H_4)W\text{–}W(CO)_2(\eta^5\text{-}C_5H_5)$ can be formed efficiently. Thus, the inability to form a W–W-bonded species upon irradiation of the surface-confined species alone suggests that the surface species are geometrically constrained. Similarly, we note that thermolysis of $(\eta^5\text{-}C_5H_5)W(CO)_3C_2H_5$ (145 °C, 3 h, sealed tube, under Ar) leads to complete loss of starting material and a good yield of $(\eta^5\text{-}C_5H_5)_2W_2(CO)_6$. By way of contrast, thermolysis of $[SiO_2]\text{–}SiMe_2\text{–}(\eta^5\text{-}C_5H_4)W(CO)_3C_2H_5$ under the same conditions and for the same time yields no detectable W–W-bonded species, significant unreacted starting material, and some new surface metal carbonyl that has an infrared spectrum consistent with the presence of the surface-bound ethylene–hydride. Thermolysis of $[SiO_2]\text{–}SiMe_2\text{–}(\eta^5\text{-}C_5H_4)W(CO)_3C_2H_5$ at 145 °C under a dynamic vacuum for 3 h, where volatiles such as CO and C_2H_4 can be swept away, yields complete disappearance of surface metal carbonyls. Under these conditions $(\eta^5\text{-}C_5H_5)W(CO)_3C_2H_5$ still gives a good yield of $(\eta^5\text{-}C_5H_5)_2W_2(CO)_6$. Thus, both in photochemical and thermal experiments it appears that the surface-bound complexes cannot form metal–metal bonds, in contrast to their solution analogues.

Discussion

The combination of synthetic approach, infrared and UV–vis spectroscopy, and elemental analyses establish the ability to covalently anchor $(\eta^5\text{-}C_5H_5)W(CO)_3R$ species to $[SiO_2]$– and $[P]\text{–}CH_4CH_2Cl$ surfaces. Quantitation of surface coverage, however, is relatively poor, that is, to within a factor of 2 or 3 in most cases which is sufficient for many applications. Errors in quantitative infrared determinations arise predominantly from two factors, solid-state effects and scattering. It is well established that CO infrared stretches for metal carbonyls are extremely sensitive to solvent and that solid-state spectra tend to be distorted compared to solution spectra;[26] the use of these spectra for quantitative analysis can thus be questioned. The surface-supported species infrared spectra accord well with the analogous solution species, Table I. However, coverage calculations based on extinction coefficients for solution species result in coverages which are too low by a factor of 10–20 as compared to elemental analysis. This can be understood by considering that when spectra of particulate samples (>μm for IR analysis) such as surface-supported species are obtained a significant amount of scattering occurs. (Uncorrected base-line absorbances of 1.0 are typical, corresponding to 90% of the light being scattered.) The net result is that some of the absorbing species are blocked from the light and do not contribute to the measured absorbance. A lower absorbance per unit

---

(26) Braterman, P. S. *Struct. Bonding (Berlin)* **1976**, *26*, 1.

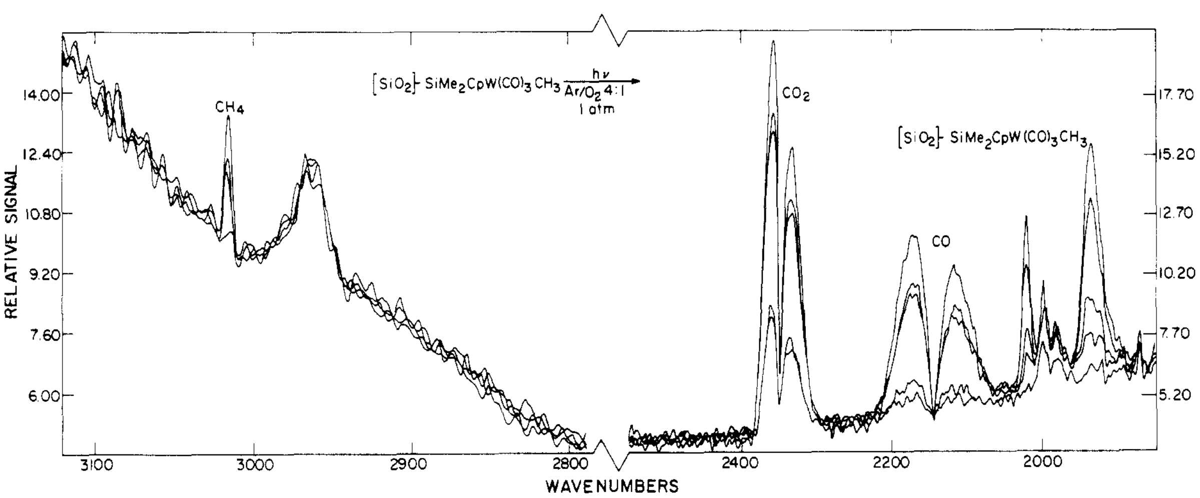

Figure 9. Infrared spectral changes monitored by FTIR/PAS accompanying the irradiation of $[SiO_2]$–$SiMe_2$–(η^5-C_5H_4)$W(CO)_3CH_3$ in 4:1 Ar/O_2. The disappearance of all metal carbonyl bands occurs upon irradiation along with the appearance of CO_2, CO, and CH_4 in the gas phase.

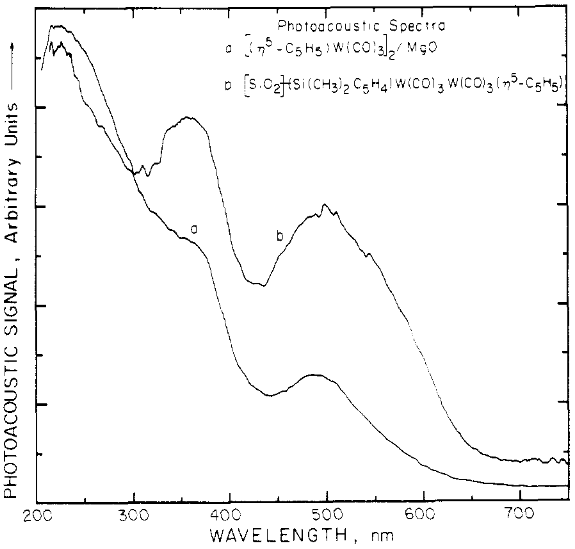

Figure 10. UV–vis photoacoustic spectrum of $[SiO_2]$-bound material from irradiation of $[SiO_2]$–$SiMe_2$–(η^5-C_5H_4)$W(CO)_3C_2H_5$ suspended in a THF solution of (η^5-C_5H_5)$W(CO)_3C_2H_5$ compared to a spectrum for authentic (η^5-C_5H_5)$_2W_2(CO)_6$ diluted with MgO.

molecule is observed as compared to solution species. Thus, we have used a KBr pellet as the medium to obtain intensity information for metal carbonyls to compare with surface-confined species. Such data yield coverage within a factor of 2 or 3 of those obtained by elemental analyses. Elemental analysis will probably remain the most definitive method to determine surface coverage; however, infrared analysis can be used as a quantitative tool for strictly defined samples. Clearly, the spectral features themselves, Figures 1–8, are quite similar for either pure or surface-confined species when similar solvents are used.

Reactivity of the surface-bound species for the most part parallels the reactivity of solution species. Loss of CO is the primary result of photoexcitation as shown by photosubstitution experiments and by direct spectroscopic characterization of the photogenerated 16-valence-electron species at low temperatures. It should be noted that there appears to be little evidence for reaction of this reactive species with the support (either $[SiO_2]$– or [P]–$C_6H_4CH_2Cl$) at any temperature used. Presumably the mode of surface anchoring through the cyclopentadienyl ring is sufficiently removed from the W center that the unsaturated species behaves as its solution analogue. The photogenerated 16-valence-electron species does react with oxygen leading to formation of CO_2 presumably by oxidation of bound CO.

Major differences in reactivity of surface-immobilized and solution species are observed when considering reactions involving two tungsten centers. The lack of W–W dimer formation, thermally or photochemically, represents the major difference in reactivity of the surface-immobilized species compared to solution species. The mean distance between tungsten centers is ~10–20 Å for the SiO_2-supported species, Table II, which is much larger than 3.22 Å, the W–W distance in (η^5-C_5H_5)$_2W_2(CO)_6$.[27] Formation of dimer from two surface species is prevented by geometrical constraints and not by inherent reactivity differences since we find efficient formation of "one side" bound dimer upon irradiation of a mixture of surface-bound and solution (η^5-C_5H_5)$W(CO)_3C_2H_5$.

Both polymer-bound and solution η^1-benzyl species react rapidly to give η^3-benzyl species upon photoinduced loss of CO. Although the photoinduced formation of solution η^3-benzyl species is well established,[28] no data existed concerning the kinetic parameters of formation. X-ray diffraction and infrared data for (η^5-C_5H_5)$Mo(CO)_2$(η^3-$CH_2C_6H_4CH_3$),[23,29] have established that the stable conformation of the η^3-benzyl is the one where the phenyl ring is down away from the cyclopentadienyl ring as shown in A. The other possible configuration shown in structure B is predicted to have a pair of carbonyl stretches in the infrared at slightly lower energy than those observed for A on the basis of infrared and NMR studies on the analogous η^3-allyl and substituted allyl species.[23] The infrared spectrum of the (η^5-C_5H_5)$W(CO)_2$(η^3-$CH_2C_6H_5$) formed at 77 K, Figure 6a, suggests that both configurations A and B are formed at low temperature, since the

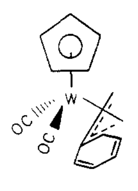

A

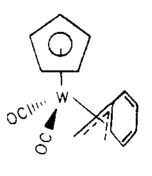

B

---

[27] Adams, R. D.; Collins, D. H.; Cotton, F. A. *Inorg. Chem.* **1974**, *13*, 1086.

[28] King, R. B.; Fronzaglia, A. *J. Am. Chem. Soc.* **1966**, *88*, 709.

[29] Cotton, F. A.; LaPrade, M. D. *J. Am. Chem. Soc.* **1968**, *90*, 5418.

Scheme I. Proposed Mechanism for Isomerization of Alkyl Group in the Photogenerated (η^5-C_5H_5)W(CO)$_2$CH$_2$CH$_2$C$_6$H$_5$

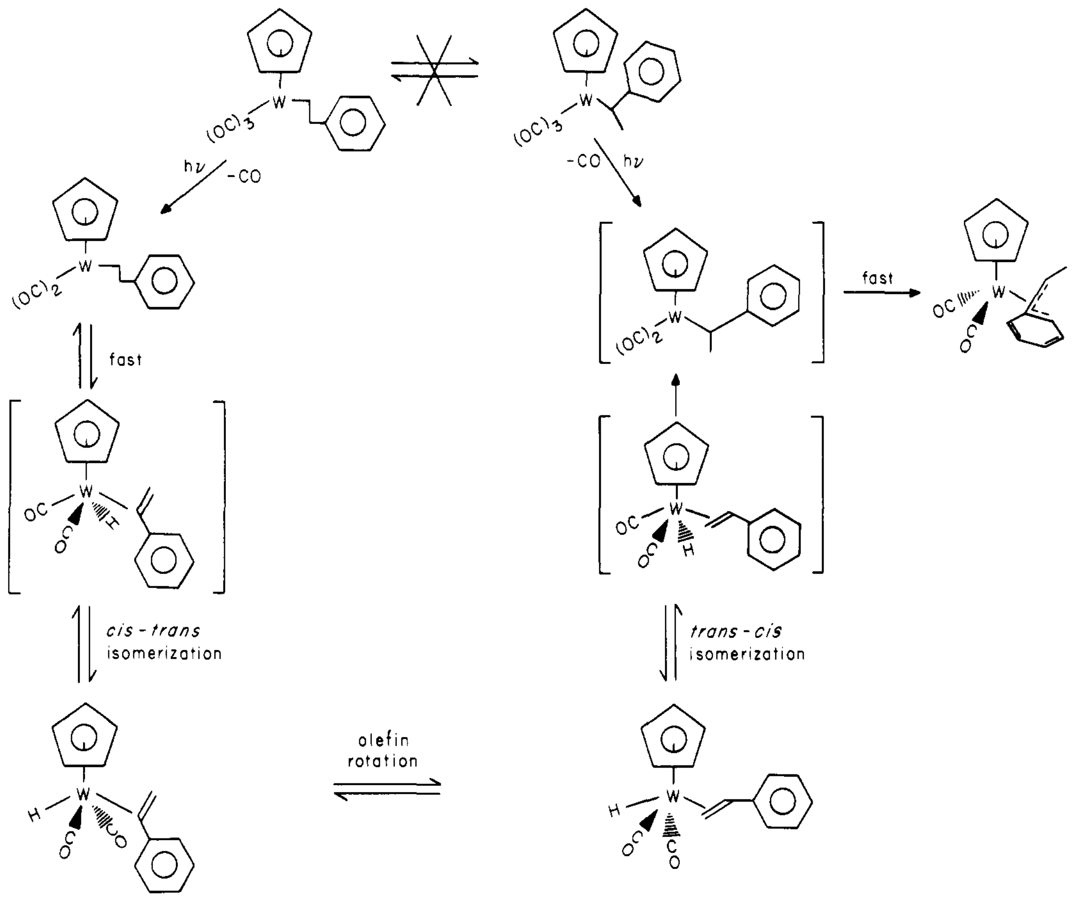

1863-cm^{-1} peak has a shoulder at 1855 cm^{-1}. The (η^5-C_5H_5)W(CO)$_2$(η^3-CH(CH$_3$)C$_6$H$_5$) also shows additional peaks at lower energy peaks at low temperatures. For both η^3-CH$_2$C$_6$H$_5$ and η^3-CH(CH$_3$)C$_6$H$_5$ warming to 298 K results in the disappearance of the peaks at ~1855 cm^{-1} and growth in ~1865-cm^{-1} peaks consistent with the presence of only isomer A at 298 K. However, the [P]–C$_6$H$_4$CH$_2$-bound species, Figure 6b, may exist entirely in the B configuration possibly due to steric constraints within the polystyrene matrix. This conclusion is drawn because the CO stretching frequencies are somewhat lower in energy than for the solution species.

The η^3-benzyl ligand is fluxional on the NMR time scale[30] leading to exchange between two halves of the benzyl and also between both faces. This exchange has been proposed to occur via a change to η^1 coordination, rotation of the benzyl ligand about the C$_1$–C$_7$ bond, and recoordination in an η^3 fashion. The reported activation energy of 15.9 ± 0.2 kcal/mol presumably corresponds to the conversion of η^3- to η^1-benzyl as the rate-determining step.

The results presented here establish an upper limit of ~6 kcal/mol for the reverse process, η^1- to η^3-benzyl conversion. The very low activation energy for this process is also illustrated in the experiments with (η^5-C_5H_5)W(CO)$_3$(η^1-CH(CH$_3$)C$_6$H$_5$). Since the alkyl group contains both a benzyl functionality and β-ydrogens, loss of CO leads to either η^3-benzyl formation or formation of a β-C–H interaction. The experiments, Figures 7b and 8, show that $\eta^{3'}$-benzyl formation is the preferred path at a temperature as low as 77 K.

The observation of (η^5-C_5H_5)W(CO)$_2$CH$_2$CH$_2$C$_6$H$_5$ upon irradiation of the parent tricarbonyl at 77 K establishes that isomerization of the alkyl group via a series of β-hydrogen transfer does not occur at this temperature since any (η^5-C_5H_5)W(CO)$_2$(η^1-CH(CH$_3$)C$_6$H$_5$) that formed would rapidly rearrange to form the stable η^3 species. (η^5-C_5H_5)W(CO)$_2$(H)(styrene) is observed upon warming from 77 K or upon irradiation of the parent tricarbonyl at 195, 273, or 300 K in fluid or solid (paraffin) solution. The subsequent thermal reaction which converts the styrene–hydride to the η^3-CH(CH$_3$)C$_6$H$_5$ species, eq 22, is best accounted for by considering Scheme I.

Based on the reactions of other W species containing β-hydrogens,[14] one predicts that the photogenerated 16-valence-electron dicarbonyl alkyl is in rapid equilibrium with the *cis*-styrene–hydride which slowly isomerizes to the relatively inert *trans*-styrene–hydride with a rate of approximately 0.05 s^{-1} at 195 K and an activation energy of ~10 kcal/mol. The rate of olefin rotation is proposed to be slower than cis → trans isomerization on the basis of variable-temperature ^{1}H NMR studies[31] for (η^5-C_5H_5)W(CO)$_2$(ethylene)CH$_3$ where an activation energy of 14.1 kcal/mol was reported although the exact mode of olefin binding is not known. The activation energy for rotation of the styrene may be higher due to its larger size.

At the *trans*-styrene–hydride stage olefin rotation can occur since the subsequent step, trans → cis isomerization, is even slower. The limiting rate for PPh$_3$ reaction with *trans*-(η^5-C_5H_5)W(CO)$_2$(H)(pentene) to form (η^5-C_5H_5)W(CO)$_2$(PPh$_3$)(*n*-pentyl) is 1.7 × 10^{-3} s^{-1} at 298 K and involves trans–cis isomerization as the rate-determining step. The rate of trans → cis isomerization is unlikely to be affected significantly by substitution of styrene for pentene, since studies of cis–trans isomerization for a series of

---

[30] Cotton, F. A.; Marks, T. J. *J. Am. Chem. Soc.* **1969**, *91*, 1339.

[31] Alt, H. G.; Schwarzle, J. A.; Kreiter, C. G. *J. Organomet. Chem.* **1978**, *153*, C7.

(η^5-C_5H_5)Mo(CO)$_2$(L)H (L = phosphine or phosphite) species show only small variations with changes in L.[32] The *cis*-styrene hydride formed at this point can have a different orientation of the styrene relative to the metal allowing transfer of the hydrogen to the terminal carbon resulting in (η^5-C_5H_5)W(CO)$_2$(η^1-CH(CH_3)C_6H_5) that rapidly forms the corresponding η^3 18-valence-electron species. It should be noted that previous studies on (η^5-C_5H_5)W(CO)$_3$$CH_2CD_3$ and the –CD_2CH_3 compound have shown that scrambling of α- and β-carbon can occur faster than formation of *trans*-alkene hydride. In that case the smaller olefin ethylene apparently can rotate faster than cis to trans isomerization occurs.

Acknowledgment. B.K. thanks the Swiss National Science Foundation for support as a Postdoctoral Fellow, 1980–1981. Support of the National Science Foundation by grant support is gratefully acknowledged. We thank the National Institutes of Health (Grant GM27551) for the Nicolet 7199 FTIR used in these studies.

Registry No. (η^5-C_5H_5)W(CO)$_3$$CH_3$, 12082-27-8; HSiMe$_2$–($\eta^5$-$C_5H_4$)W(CO)$_3$$CH_3$, 82615-15-4; $C_6H_5CH_2$–(η^5-C_5H_4)W(CO)$_3$$CH_3$, 82615-16-5; ($\eta^5$-$C_5H_5$)W(CO)$_2$$CH_3$, 73715-35-2; HSiMe$_2$–($\eta^5$-$C_5H_4$)W(CO)$_2$$CH_3$, 82615-17-6; ($\eta^5$-$C_5H_5$)W(CO)$_2$(PPh$_3$)$CH_3$, 12115-41-2; HSiMe$_2$–($\eta^5$-$C_5H_4$)W(CO)$_2$(PPh$_3$)$CH_3$, 82615-18-7; ($\eta^5$-$C_5H_5$)W(CO)$_3$$C_2H_5$, 51232-59-8; ASiMe$_2$–($\eta^5$-$C_5H_4$)W(CO)$_3$$C_2H_5$, 82615-19-8; $C_6H_5CH_2$–(η^5-C_5H_4)W(CO)$_3$$C_2H_5$, 82615-20-1; ($\eta^5$-$C_5H_5$)W(CO)$_2$$C_2H_5$, 82615-21-2; ASiMe$_2$–($\eta^5$-$C_5H_4$)W(CO)$_2$$C_2H_5$, 82615-22-3; ($\eta^5$-$C_5H_5$)W(CO)$_2$(PPh$_3$)$C_2H_5$, 82615-23-4; HSiMe$_2$–($\eta^5$-$C_5H_4$)W(CO)$_2$(PPh$_3$)$C_2H_5$, 82615-24-5; ($\eta^5$-$C_5H_5$)W(CO)$_2$(H)($C_2H_4$), 80376-16-5; HSiMe$_2$–($\eta^5$-$C_5H_4$)W(CO)$_2$(H)($C_2H_4$), 82615-25-6; ($\eta^5$-$C_5H_5$)W(CO)$_3$($\eta^1$-$CH_2C_6H_5$), 38547-50-1; ($\eta^5$-$C_5H_5$)W(CO)$_3$($\eta^3$-$CH_2C_6H_5$), 82615-26-7; ($\eta^5$-$C_5H_5$)W(CO)$_2$(PPh$_3$)($\eta^1$-$CH_2C_6H_5$), 81371-86-0; ($\eta^5$-$C_5H_5$)W(CO)$_3$$CH_2CH_2C_6H_5$, 82615-27-8; ($\eta^5$-$C_5H_5$)W(CO)$_2$$CH_2CH_2C_6H_5$, 82615-28-9; ($\eta^5$-$C_5H_5$)W(CO)$_2$(PPh$_3$)$CH_2CH_2C_6H_5$, 82615-29-0; ($\eta^5$-$C_5H_5$)W(CO)$_2$(H)(styrene), 82615-30-3; (η^5-C_5H_5)W(CO)$_3$(η^1-CH(CH_3)C_6H_5), 82615-31-4; (η^5-C_5H_5)W(CO)$_2$(PPh$_3$)(η^1-CH(CH_3)C_6H_5), 82615-32-5; (η^5-C_5H_5)W(CO)$_2$(η^3-CH(CH_3)C_6H_5), 82615-33-6; (η^5-C_5H_5)W(CO)$_3$Cl, 12128-24-4; HSiMe$_2$–(η^5-C_5H_4)W(CO)$_3$Cl, 82615-34-7; (η^5-C_5H_5)W(CO)$_2$(PPh$_3$)Cl, 12115-03-6; HSiMe$_2$-(η^5-C_5H_4)W(CO)$_2$(PPh$_3$)Cl, 82615-35-8.

---

[32] Faller, J. W.; Anderson, A. S. *J. Am. Chem. Soc.* **1970,** *92,* 5852.

Chemistry of Octacarbonyl(μ-methylene)diiron and Its Derivatives

Charles E. Sumner, Jr.,*[†] Joseph A. Collier,[‡] and R. Pettit[§]

Department of Chemistry, The University of Texas at Austin, Austin, Texas 78712

Received January 7, 1982

The reaction of the $Fe_2(CO)_8^{2-}$ dianion with methylene iodide leads to the formation of the parent bridging methylene complex, octacarbonyl(μ-methylene)diiron, $Fe_2(CO)_8CH_2$. The reaction appears to be general and several derivatives have been prepared by using other geminal diiodides. The bridging methylene complexes react with unsaturated reactants such as olefins and acetylenes to produce new organometallic complexes in which the unsaturated molecule has inserted between the methylene ligand and an iron atom. With hydrogen, the complexes react to produce the dihydro form of the methylene ligand; nucleophilic reagents such as iodide ion, alcohols, and water appear to attack a CO ligand with subsequent rearrangement involving the bridging methylene group.

Introduction

In addition to their interest from a structural point of view, organometallic complexes containing carbon ligands have been implicated as intermediates in several important chemical reactions, e.g., the disproportionation of olefins[1] and the Fischer–Tropsch reaction,[2] and the chemistry of such species has emerged as an important area of study. In this paper we discuss the preparation and chemical properties of octacarbonyl(μ-methylene)diiron and several of its derivatives.

Discussion

We recently reported the synthesis of the parent μ-methylene complex $Fe_2(CO)_8CH_2$[3] by the reaction of $(Et_4N)_2Fe_2(CO)_8$ with CH_2I_2 (eq 1). We have found the

$$(Et_4N)_2Fe_2(CO)_8 + CH_2I_2 \rightarrow Fe_2(CO)_8CH_2 \quad (1)$$

reaction of geminal diiodoalkanes with $(Et_4N)_2Fe_2(CO)_8$ to be a general synthesis of diiron μ-alkylidene complexes. For example, treatment of $(Et_4N)_2Fe_2(CO)_8$ with 1,1-diiodoethane affords the μ-ethylidene complex **2** (eq 2).

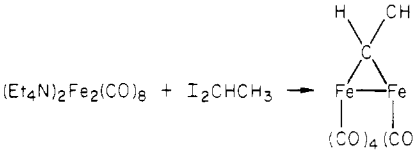

$$(Et_4N)_2Fe_2(CO)_8 + I_2CHCH_3 \rightarrow (CO)_4Fe(\mu\text{-}C(H)CH_3)Fe(CO)_4 \quad (2)$$

2

Similar results are obtained when 2,2-diiodopropane, 1,1-diiodo-2-methyl propane, α,α-diiodoethyl acetate, or diiodopropene[4] is substituted for CH_2I_2. The μ-alkylidene complexes obtained from these diiodides are listed in Table I along with their spectroscopic data. The use of the disodium salt of $[Fe_2(CO)_8]^{2-}$ in place of the tetraethyl-

---

[†] Tennessee Eastman Co., P.O. Box 511, Kingsport, TN 37662.

[‡] Union Carbide Corp., South Charleston, WV 25303.

[§] Deceased December 10, 1981.

(1) Calderon, N.; Ofstead, E. A.; Judy, W. A. *Angew. Chem., Int. Ed. Engl.* **1976,** *15,* 401.

(2) Brady, R. C., III; Pettit, R. *J. Am. Chem. Soc.* **1981,** *103,* 1287.

(3) Sumner, C. E., Jr.; Riley, P. E.; Davis, R. E.; Pettit, R. *J. Am. Chem. Soc.* **1980,** *102,* 1752.

(4) Used as a mixture of compounds prepared by the reaction of vinyldiazomethane with iodine.

0276-7333/82/2301-1350$01.25/0